Journal of Medicinal Chemistry

ARTICLE

pubs.acs.org/jmc

Structure-Guided Lead Optimization of Triazolopyrimidine-Ring Substituents Identifies Potent *Plasmodium falciparum* Dihydroorotate Dehydrogenase Inhibitors with Clinical Candidate Potential

Jose M. Coteron,[§] María Marco,[§] Jorge Esquivias,[§] Xiaoyi Deng,[†] Karen L. White,[∥] John White,[⊥] Maria Koltun,[∥] Farah El Mazouni,[†] Sreekanth Kokkonda,[⊥] Kasiram Katneni,[∥] Ravi Bhamidipati,[∥] David M. Shackleford,[∥] Iñigo Angulo-Barturen,[§] Santiago B. Ferrer,[§] María Belén Jiménez-Díaz,[§] Francisco-Javier Gamo,[§] Elizabeth J. Goldsmith,[‡] William N. Charman,[∥] Ian Bathurst,[#] David Floyd,[#] David Matthews,[#] Jeremy N. Burrows,[#] Pradipsinh K. Rathod,[⊥] Susan A. Charman,[∥] and Margaret A. Phillips*[,†]

[†]Department of Pharmacology and [‡]Biochemistry, University of Texas Southwestern Medical Center at Dallas, 6001 Forest Park Rd, Dallas, Texas 75390-9041, United States

[§]GlaxoSmithKline, Diseases of the Developing World (DDW)—Tres Cantos Medicines Development Campus, Madrid, Spain

[∥]Centre for Drug Candidate Optimisation, Monash Institute of Pharmaceutical Sciences, Monash University (Parkville Campus), Parkville, VIC 3052, Australia

[⊥]Departments of Chemistry and Global Health, University of Washington, Seattle, Washington 98195, United States

[#]Medicines for Malaria Venture, Geneva, Switzerland

Supporting Information

ABSTRACT: Drug therapy is the mainstay of antimalarial therapy, yet current drugs are threatened by the development of resistance. In an effort to identify new potential antimalarials, we have undertaken a lead optimization program around our previously identified triazolopyrimidine-based series of *Plasmodium falciparum* dihydroorotate dehydrogenase (*Pf*DHODH) inhibitors. The X-ray structure of *Pf*DHODH was used to inform the medicinal chemistry program allowing the identification of a potent and selective inhibitor (DSM265) that acts through DHODH inhibition to kill both sensitive and drug resistant strains of the parasite. This compound has similar potency to chloroquine in the humanized SCID mouse *P. falciparum* model, can be synthesized by a simple route, and rodent pharmacokinetic studies demonstrated it has excellent oral bioavailability, a long half-life and low clearance. These studies have identified the first candidate in the triazolopyrimidine series to meet previously established progression criteria for efficacy and ADME properties, justifying further development of this compound toward clinical candidate status.

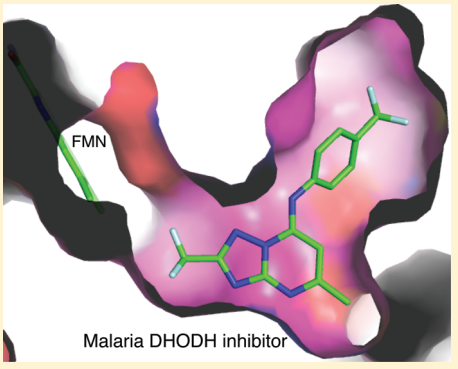

INTRODUCTION

Malaria is an ancient human enemy with descriptions of malarial-like febrile illness documented over 2000 years ago in the writings of the Greek physician Hippocrates.[1] The identification of the parasite and the link to mosquito-based transmission in 1880 led to our modern understanding of the disease. Drugs to treat malaria predate our knowledge of its etiology (e.g., quinine was isolated from the cinchona bark in 1820), yet today malaria still leads to 220 million cases and approximately 1 million deaths per year, with over 2 billion people at risk for the disease.[2,3] The world community is currently involved in its second attempt at global malaria eradication.[4] While some progress has been made in developing a vaccine, the best candidate RTSS provides only partial immunity.[5] Thus the mainstay of antimalarial treatment and the key to successful eradication continues to be chemotherapy. Against a backdrop of widespread drug resistance to traditional therapies (e.g., chloroquine and pyrimethamine/sulfadoxine), the introduction of artemisinin-based combination therapies (ACTs) has become the most powerful tool to combat the disease.[6,7] ACTs are highly effective for the treatment of *Plasmodium falciparum* malaria leading to significant reduction in the mortality and morbidity of the disease. Recent emergence of potential artemisinin resistance along the Thai−Cambodia border threatens to derail these successes, as well as any hope at global eradication.[8] Few clinically approved treatment options will remain if artemisinin resistance becomes widespread.

A continual pipeline to identify and develop antimalarial agents is required to combat the ability of the parasite to rapidly

Received: May 11, 2011
Published: June 22, 2011

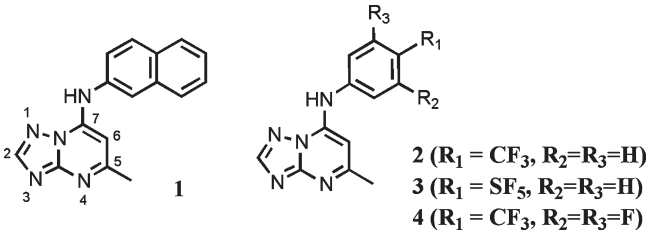

Figure 1. Structures of select triazolopyrimidines.

acquire resistance to chemotherapy in the field.[9] The global effort to identify new drugs is being fueled by not-for-profit organizations and the development of substantial portfolios of candidate molecules ranging from identified hits to compounds in clinical development.[10−12] The completion of whole organism screens of large chemical libraries has identified thousands of new chemical species with antimalarial activity,[13,14] while target-based approaches are also being successfully used to find novel chemotypes. The translation of these findings to clinical successes still presents a formidable challenge to the development of new drugs.

Dihydroorotate dehydrogenase (DHODH) has emerged as the best validated new target for the development of novel antimalarials since the identification of the bc1 complex as the target of atovaquone, due to the discovery of several classes of inhibitors with antimalarial activity.[15] DHODH catalyzes the fourth step in the de novo pyrimidine biosynthetic pathway, the flavin mononucleotide (FMN)-dependent oxidation of dihydrorotate to orotic acid. *P. falciparum* DHODH (*Pf*DHODH) is localized to the inner mitochondrial-membrane and utilizes ubiquinone (CoQ) as the final electron acceptor to regenerate oxidized FMN. The malaria parasite is uniquely vulnerable to inhibition of this pathway because it lacks the salvage enzymes that serve as an additional source of pyrimidine nucleosides in other organisms, including the human host. Several different chemical series that are potent inhibitors of *Pf*DHODH have been identified by enzyme activity-based HTS and were subsequently found to have antimalarial activity both in vitro and in vivo. These include the triazolopyrimidines (**1**) (Figure 1) identified by our group[16−19] and *N*-alkyl-5-(1*H*-benzimidazol-1-yl)-thiophene-2-carboxamides identified by Genzyme and colleagues.[20,21] Structural analysis of the bound inhibitor enzyme complexes has revealed that these different chemical classes have overlapping but distinctly different binding modes owing to conformational flexibility in the enzyme inhibitor binding site.[21,22] Most recently, metabolically stable triazolopyrimidines (**2**−**4**) (Figure 1) have been identified that are able to suppress parasites in a mouse model of infection, however these compounds lacked the potency required in a clinical development candidate.[16,19] To improve the potency of the series, we have utilized the X-ray structural information to guide additional medicinal chemistry. The enzyme bound structure of **1** and **2** showed that the triazolopyrimidines filled most of the available binding pocket but that a channel between the C2 position of the triazolopyrimidine ring and the FMN cofactor was available that could potentially accommodate additional functionality.[22] In a major advance forward, herein we describe the lead optimization program to modify the C2 position of the triazolopyrimidine scaffold that has yielded several potent compounds with pharmacokinetic profiles and in vivo efficacy in mouse models that meet previously established progression criteria.

CHEMISTRY

The focus of this study was to examine the SAR associated with modifications of the substituent at C2 of the triazolopyrimidine ring system. The development of a synthetic strategy for these triazolopyrimidine derivatives was dictated by the nature of the atom used as linker at the C2- position of the ring. The synthesis of the 2-substituted analogues **11**−**55** shown in Table 1 proceeded through the intermediate 7-hydroxy-triazolopyrimidines **9** shown in Scheme 1, which was accessed by two routes. The most general approach involved the condensation of ethyl 3-oxobutanoate with aminoguanidine hydrochloride to afford diaminopyrimidone **7** in moderate yield (**11**−**42** and **45**−**55**). This route had the advantage that **7** served as a common intermediate from which a diverse set of C2 alkyl analogues could be prepared. Reaction of **7** with a variety of acid chlorides (R defined in Table 1) gave the C2 substituted triazolopyrimidones **9** in good to excellent yields, even with sterically hindered R groups. This reaction apparently proceeded by initial acylation of **7** followed by a slower cyclization step yielding **9** and, in some cases, required more forcing conditions to effect complete conversion to **9**.[23] Alternatively, to generate **43**, **44**, and **100**, we used our previously described chemistry[16,17,19] in which the 5-aminotriazoles **8** were either commercially available or prepared initially (see Materials and Methods). In these cases, the reaction of **8** with ethyl 3-oxobutanoate proceeded through the acetoacetate ketone with formation of an aminocrotonate intermediate that cyclizes at the N-2 of the triazole ring yielding the desired isomer **9**.[24,25] The limitation of this approach was the availability of starting 3-substituted-5-amino-1,2,4-triazole derivatives due to lengthy reaction times, inefficiency and variable results during their preparation. Treatment of **9** with phosphoryl chloride then gave the chloro triazolopyrimidines **10**, which could be converted to the desired 2-substituted 7-aminoaryl products **11**−**55**, **100** by reaction with the requisite aniline under a variety of conditions.

As shown in Scheme 2, the preparation of analogues with either S- or O-linked substituents at C2 (**58**−**84**) started with the commercially available triazolopyrimidone **56**. Conversion of **56** to the chloride (**57**, R = SMe) under the standard conditions followed by displacement of the chloro group with the requisite aniline afforded compounds **58**−**61** in good yields. Oxidation with hydrogen peroxide in the presence of catalytic Na_2WO_4 in hot aqueous acetic acid proved to be very straightforward, although competitive nitrogen oxidation lowered the yield of this step. Nevertheless, compounds **62**−**65** were easily prepared by this procedure. These compounds then served as intermediates for the preparation of compounds **66**−**84** by taking advantage of the methylsulfonyl group to act as a leaving group. Thus, treatment of these C2 methylsulfonyl analogues with a variety of alkyl and functionalized alkyl alkoxides under microwave conditions afforded the desired compounds (**66**−**84**) in good yields.

Analogues with amino (**89**−**97**) or hydroxyl (**98**, **99**, **101**) functionality at the R position were obtained from specific intermediates **45**−**47** (prepared as in Scheme 1) and further derivatized as shown in Schemes 3 and 4. Compounds **89**−**97** were generated in moderate to good yields by treating the fully elaborated chloromethyl (**45a**, **45b**) or chloroethyl (**46a**, **46b**) analogues with the appropriate amine in methanol or THF in the microwave at 120 °C (Scheme 3). The hydroxyl alkyl analogues **98**−**99**, **101** were prepared by hydrogenolysis (Scheme 4) of the requisite benzyl ether (**47a**, **47b**) using flow chemistry with an H-cube instrument.

Table 1. Structure−Activity Relationships of the Triazolopyrimidine Compounds[a]

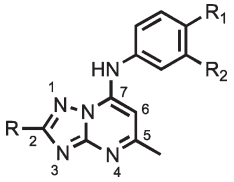

compd	name	R	R1	R2	IC_{50} (μM) *Pf*DHODH	IC_{50} (μM) *Pb*DHODH	IC_{50} (μM) *h*DHODH	EC_{50} (μM) *Pf* 3D7 cells
2	DSM74[b]	H	CF_3	H	0.28	0.38	>100	0.34
3	DSM161[c]	H	SF_5	H	0.13	0.28	>100	1.3, 0.18*
5	DSM89	H	Cl	H	1.6	5.7	>100	12
6	DSM75	H	H	Cl	1.4	31	>100	8.5
11	DSM271	CH_2CH_3	Cl	H	0.28	2.3	ND	0.79
12	DSM272	CH_2CH_3	H	Cl	0.24	ND	ND	3.3
13	DSM280	CH_2CH_3	CF_3	H	0.087	0.76	>100	0.058
14	DSM281	CH_2CH_3	SF_5	H	0.15	1.4	>100	0.1
15	DSM309	*iso*-Pr	Cl	H	0.33	2.1	ND	0.85
16	DSM308	*iso*-Pr	H	Cl	0.12	0.57	ND	1.1
17	DSM307	*iso*-Pr	CF_3	H	0.11	4.5	>100	0.098
18	DSM314	*iso*-Pr	SF_5	H	0.10	3.8	>100	0.42
19	DSM313	*iso*-Bu	Cl	H	>10	ND	ND	ND
20	DSM312	*iso*-Bu	H	Cl	>10	ND	ND	ND
21	DSM311	*iso*-Bu	CF_3	H	2.0	ND	ND	ND
22	DSM310	*iso*-Bu	SF_5	H	>10	ND	ND	ND
23	DSM357	*tert*-Bu	CF_3	H	0.46	15	>100	0.29
24	DSM358	*tert*-Bu	SF_5	H	0.55	16	>100	2.3
25	DSM356	*sec*-Bu	CF_3	H	0.38	4.6	>100	0.27
26	DSM355	*sec*-Bu	SF_5	H	0.33	4.5	>100	0.51
27	DSM325	cycloPr	Cl	H	0.88	2.8	>100	6.8
28	DSM324	cycloPr	H	Cl	0.82	1.7	>100	ND
29	DSM322	cycloPr	CF_3	H	0.14	2.6	>100	0.15
30	DSM323	cycloPr	SF_5	H	0.093	2.0	>100	0.50
31	DSM321	CH_2cycloPr	Cl	H	12	ND	ND	ND
32	DSM320	CH_2cycloPr	H	Cl	>10	ND	ND	ND
33	DSM318	CH_2cycloPr	CF_3	H	1.7	ND	ND	3.4
34	DSM319	CH_2cycloPr	SF_5	H	5.7	ND	ND	>10
35	DSM254	CF_2CH_3	Cl	H	0.038	1.7	>100	0.050
36	DSM266	CF_2CH_3	H	Cl	0.054	ND	ND	0.13
37	DSM267	CF_2CH_3	CF_3	H	0.038[d]	2.4	>100	0.010[f]/0.0062*
38	DSM265	CF_2CH_3	SF_5	H	0.033[e]	2.5	>100	0.046[g]/0.0078*
39	DSM329	$CF_2CH_2CH_3$	Cl	H	0.034	1.8	>100	0.094
40	DSM328	$CF_2CH_2CH_3$	H	Cl	0.030	1.4	>100	1.2
41	DSM326	$CF_2CH_2CH_3$	CF_3	H	0.019	2.5	>100	0.045
42	DSM327	$CF_2CH_2CH_3$	SF_5	H	0.075	4.7	>100	0.55
43	DSM195	CF_3	CF_3	H	0.035	1.3	>100	0.073
44	DSM196	CF_3	SF_5	H	0.030	2.5	41	0.14
48	DSM299	CH_2OCH_3	Cl	H	2.2	ND	ND	ND
49	DSM300	CH_2OCH_3	H	Cl	1.7	ND	ND	ND
50	DSM305	CH_2OCH_3	CF_3	H	0.41	5.5	ND	1.0
51	DSM306	CH_2OCH_3	SF_5	H	0.39	3.3	ND	2.1
52	DSM301	$CH_2CH_2OCH_3$	Cl	H	>10	ND	ND	ND
53	DSM302	$CH_2CH_2OCH_3$	H	Cl	>10	ND	ND	ND
54	DSM303	$CH_2CH_2OCH_3$	CF_3	H	2.5	ND	ND	4.2
55	DSM304	$CH_2CH_2OCH_3$	SF_5	H	2.5	ND	ND	5.0
58	DSM257	SCH_3	Cl	H	0.030	ND	ND	0.15

dx.doi.org/10.1021/jm200592f |*J. Med. Chem.* 2011, 54, 5540–5561

Table 1. Continued

compd	name	R	R1	R2	IC_{50} (μM) *Pf*DHODH	IC_{50} (μM) *Pb*DHODH	IC_{50} (μM) *h*DHODH	EC_{50} (μM) *Pf* 3D7 cells
59	DSM258	SCH_3	H	Cl	0.026	ND	ND	0.15
60	DSM261	SCH_3	CF_3	H	0.036	4.8	ND	0.0084
61	DSM262	SCH_3	SF_5	H	0.030	>10	ND	0.032
62	DSM259	SO_2CH_3	Cl	H	0.045	ND	ND	1.4
63	DSM260	SO_2CH_3	H	Cl	0.16	ND	ND	>2.5
64	DSM263	SO_2CH_3	CF_3	H	0.090	ND	ND	0.17
65	DSM264	SO_2CH_3	SF_5	H	0.11	ND	ND	2.0
66	DSM227	OCH_3	H	Cl	0.50	1.3	ND	0.98
67	DSM241	OCH_3	Cl	H	0.46	1.2	ND	0.59
68	DSM245	OCH_2CH_3	H	Cl	0.40	1.9	>100	4.4
69	DSM246	OCH_2CH_3	Cl	H	0.27	1.6	>100	1.3
70	DSM293	OCH_2CH_3	CF_3	H	0.056	2.7	>100	0.058
71	DSM294	OCH_2CH_3	SF_5	H	0.057	0.47	>100	0.10
72	DSM298	$OCH_2CH_2OCH_3$	Cl	H	>10	ND	ND	ND
73	DSM315	$OCH_2CH_2OCH_3$	H	Cl	4.9	>10	ND	ND
74	DSM274	$O(CH_2)_2NHCH_3$	Cl	H	>10	ND	ND	ND
75	DSM273	$O(CH_2)_2NHCH_3$	H	Cl	>10	ND	ND	ND
76	DSM275	$O(CH_2)_2NHCH_3$	CF_3	H	>10	ND	ND	ND
77	DSM276	$O(CH_2)_2NHCH_3$	SF_5	H	>10	ND	ND	ND
78	DSM287	$O(CH_2)_2N(CH_3)_2$	Cl	H	>10	ND	ND	ND
79	DSM285	$O(CH_2)_2N(CH_3)_2$	H	Cl	>10	ND	ND	ND
80	DSM289	$O(CH_2)_2N(CH_3)_2$	CF_3	H	>10	ND	ND	ND
81	DSM291	$O(CH_2)_2N(CH_3)_2$	SF_5	H	>10	ND	ND	ND
82	DSM295	$O(CH_2)_2NH_2$	H	Cl	>10	ND	ND	ND
83	DSM296	$O(CH_2)_2NH_2$	CF_3	H	>10	ND	ND	ND
84	DSM297	$O(CH_2)_2NH_2$	Cl	H	>10	ND	ND	ND
85	DSM288	=O	Cl	H	>10	ND	ND	ND
86	DSM286	=O	H	Cl	>10	ND	ND	ND
89	DSM253	$(CH_2)_2NHCH_3$	Cl	H	>10	ND	ND	>2.5
90	DSM277	CH_2NH_2	Cl	H	>10	ND	ND	ND
91	DSM278	CH_2NHCH_3	Cl	H	>10	ND	ND	ND
92	DSM279	$CH_2NH(CH_3)_2$	Cl	H	>10	ND	ND	ND
93	DSM256	$(CH_2)_2NHCH_3$	H	Cl	>10	ND	ND	>2.5
94	DSM282	$CH_2NH(CH_3)_2$	H	Cl	>10	ND	ND	ND
95	DSM283	CH_2NH_2	H	Cl	>10	ND	ND	ND
96	DSM284	CH_2NHCH_3	H	Cl	>10	ND	ND	ND
97	DSM292	$CH_2CH_2NH_2$	Cl	H	>10	ND	ND	ND
98	DSM268	CH_2OH	Cl	H	5.3	ND	ND	>2.5
99	DSM255	CH_2OH	H	Cl	6.1	ND	ND	>10
101	DSM317	CH_2CH_2OH	CF_3	H	0.93	ND	ND	0.48

[a] *P. falciparum* 3D7 results: data collected in media containing human serum, except * where Albumax was used instead. ND, not determined. [b,c] Previously reported compounds.[16,19] Values were determined based on triplicate data points at each test concentration. [d] Average of $n = 4$ independent experiments on different synthetic batches (std dev = 0.012). [e] Average of $n = 4$ independent experiments on different synthetic batches (std dev = 0.0095). [f] Average of $n = 6$ independent experiments on different synthetic batches (std dev = 0.0045). [g] Average of $n = 6$ independent experiments on different synthetic batches (std dev = 0.013).

RESULTS

Optimization of Inhibitor Potency. The original triazolopyrimidine lead compound (**1**) was identified by HTS in a *Pf*DHODH-based enzyme activity based screen.[17] This compound was a potent and selective inhibitor of *Pf*DHODH, however it was rapidly metabolized and showed no activity against the parasite in vivo. Replacement of the naphthyl amine with para-substituted anilines led to the identification of metabolically stable analogues (e.g., **2**−**4**) that were able to suppress parasite growth in the *P. berghei* mouse model[16,19] (Figure 1). Additionally these studies identified the key anilines (4-CF_3 and 4-SF_5) that provided the optimal balance between parasite activity and metabolic stability. These compounds (**2**−**4**) however were less potent than expected of a drug candidate and required large doses for in vivo efficacy. The X-ray structures of *Pf*DHODH bound to **1** and **2** were determined, and this analysis identified a narrow channel leading from

the C2 carbon of the triazolopyrimidine ring toward the bound FMN cofactor.[22] This channel is lined by several hydrophobic side chains, the aliphatic side chain portion of Arg265 and by a single polar group: the side chain hydroxyl of Tyr528. This hydroxyl donates a hydrogen bond to the carbonyl oxygen of Gly226. In the cocrystal structure of *Pf*DHODH with **1**, but not with **2**, a single-ordered water molecule is trapped between bound inhibitor and protein on one side of the channel where it donates hydrogen bonds to the hydroxyl of Tyr528 and to N1

Scheme 1. Synthesis of the Triazolopyrimidine Compounds 11−55, 100[a]

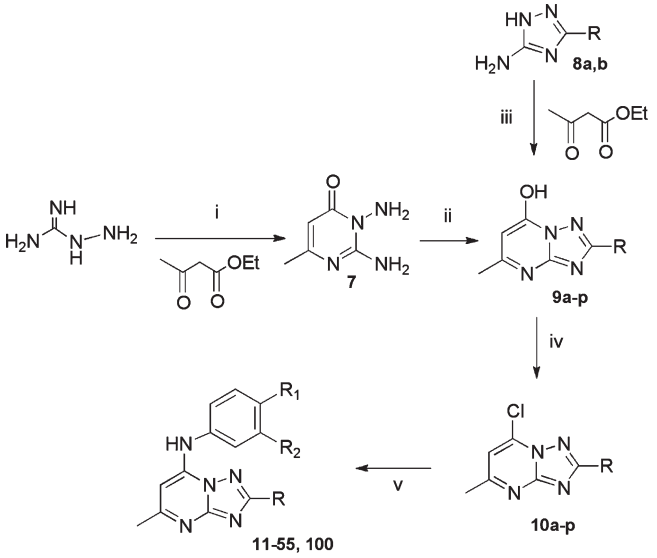

[a] General conditions: (i) EtOH, reflux 5 h, overnight at RT; (ii) **9a**−**9g**, **9j**, **9k**, **9m**−**9o**; 1,4 dioxane, DMF, requisite acid chloride, reflux O/N or **9h**, **9i**; NaEtO, EtOH, 80 °C, 30 min, appropriate difluoropropanoate or difluorobutanoate, 30 min, RT, (1.5−3) h, 80 °C; (R defined in Table 1); (iii) **9l**, **9p** AcOH, reflux, 8 h; (iv) reflux in $POCl_3$; (v) requisite aniline (R_1, and R_2 defined in Table 1), EtOH, reflux 1−3 h.

Scheme 3. Synthesis of Triazolopyrimidines 89−97[a]

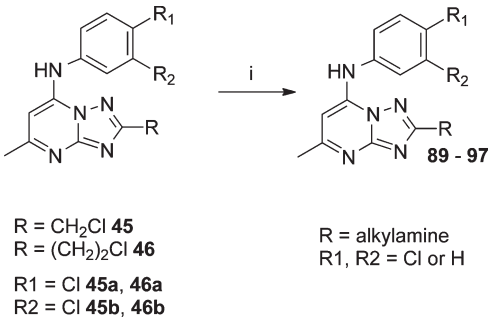

[a] Reagents and conditions: (i) amine in MeOH or THF, MW, 120 °C, 30−45 min, (40−70%).

Scheme 4. Synthesis of Triazolopyrimidines 98, 99, and 101[a]

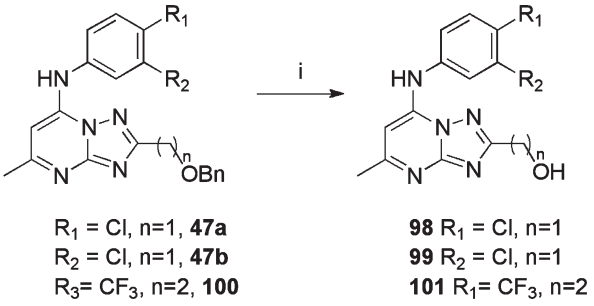

[a] Reagents and conditions: (i) Pd/C, H_2 35 psi for up to 40 h (11−12%).

Scheme 2. Synthesis of the Triazolopyrimidine Compounds 66−84[a]

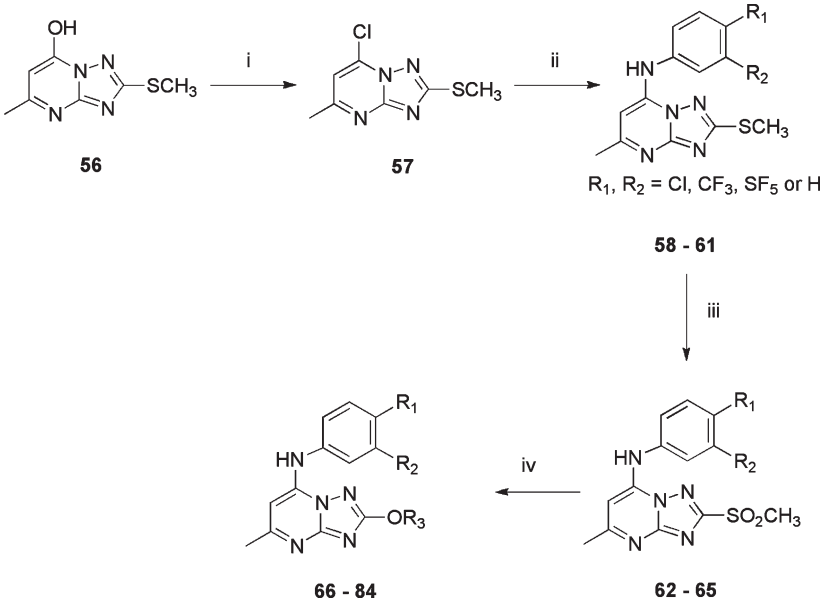

[a] General conditions: (i) $POCl_3$, reflux, 10 h; (ii) requisite aniline (R_1 and R_2 defined in Table 1), EtOH, RT; (iii) AcOH, RT, H_2O_2, Na_2WO_4 (cat), 50 °C; (iv) R_3OH (R_3 defined in Table 1), NaH, THF, microwave, 120 °C, (0.5−1) h.

dx.doi.org/10.1021/jm200592f |*J. Med. Chem.* 2011, 54, 5540–5561

of **1**. The crystal structures indicate that the triazolopyrimidine in **2** penetrates about 0.3 Å more deeply into the narrow channel than is the case with **1**, which may force a slight movement of the water molecule destabilizing its hydrogen bonding interactions and disordering its binding. To improve the potency of the compound series, we sought to exploit potential additional binding energy by building functionality from the C2 position of the ring. We reasoned that an unbranched alkyl substituent at C2 would fit well into the allowed space in the pocket. But we also recognized that protein conformational changes seen previously in *Pf*DHODH as a response to binding different inhibitor chemotypes[22] could possibly alter the shape and electronic characteristics of this narrow channel if probed by suitable C2 substituents.

To identify the most active and promising compound, we undertook a systematic evaluation of modification of the triazolopyrimidine ring at the C2 position including some larger and more polar substituents that were designed to probe the sensitivity of the channel to possible ligand induced conformational changes. The chemistry was designed to allow study of different structural effects including chain length effects, branch-group effects at different distances in C2, electronic effects on the 5-membered ring of the triazolopyrimidine, heteroatom effects at different distances in C2, polarity effects at different distances in C2, or donor and acceptor hydrogen-bonding effects in C2 looking for an extra interaction with the FMN cofactor. To evaluate whether the previously optimized anilines (4-CF_3 and 4-SF_5) remained appropriate for the various functional groups that were coupled to C2, four different anilines (4-Cl, 3-Cl, 4-CF_3, and 4-SF_5) were tested within each series.

Compounds were initially evaluated for potency against *Pf*DHODH and against the *P. falciparum* parasite in whole cell assays (Table 1). Generally, we observed a good correspondence between activity against *Pf*DHODH and inhibition of *P. falciparum* 3D7 cell growth for the compounds in the series. Alkyl R-groups at C2 were tested to explore the size of the pocket, including ethyl (**11**−**14**), *iso*-propyl (**15**−**18**), *iso*-butyl (**19**−**22**), *tert*-butyl (**23** and **24**), *sec*-butyl (**25** and **26**), and cyclopropyl (**27**−**30**). All but the *iso*-butyl substituents were tolerated and had similar activity to that of the parent compounds (**2**−**6**), with a small (2−3-fold) improvement in potency against *Pf*DHODH observed for **13**, **17**, and **29**, or a larger 5−10-fold improvement observed for the 3-Cl aniline (**12** and **16**) or the 4-Cl aniline (**11** and **15**) derivatives. These data suggest the geometry of the channel is wide enough to accept steric hindrance on the atom adjacent to the C2 carbon of the triazolopyrimidine ring but that it narrows beyond the second atom from C2. Compounds with a direct ether linkage to the triazolopyrimidine ring, OMe (**66** and **67**) and OEt (**68**−**71**), also showed similar to modestly improved potency when compared to the parent compounds (**2**−**6**). In the context of 4-CF_3− or 4-SF_5−aniline, the addition of OEt at C2 (**70** and **71**) led to 4−8-fold improved potency against *Pf*DHODH, however both were less active than those containing a haloalkyl (**37** and **38**). Addition of a linker carbon between C2 and cyclopropyl (**31**−**34**) led to reduced inhibitory activity as did increasing the chain length of the ethyl ether group at C2 (−$OCH_2CH_2OCH_3$) (**72** and **73**), demonstrating that the pocket is not able to accommodate these larger groups at the C2 position. Compounds that contained an ether linkage in the R group (**48**−**55**) that were not directly linked to the triazolopyrimidine ring showed in general lower activity than the parent compounds (**2**−**6**), as did those containing an alcohol

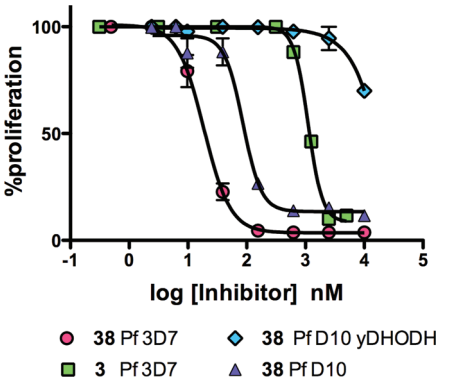

Figure 2. *P. falciparum* in vitro growth curves and genetic rescue with yeast DHODH for **38**. Data were collected in human serum and were fitted to the four-parameter dose−response equation in Graphpad Prism to obtain EC_{50} values. **38** (*P. falciparum* 3D7, EC_{50} = 0.019 μM (0.016−0.022)); **3** (*P. falciparum* 3D7, EC_{50} = 1.1 μM (1.1−1.2)); **38** (*P. falciparum* D10, EC_{50} = 0.086 μM (0.066−0.11)); **38** (*P. falciparum* D10 transfected with yeast DHODH, EC_{50} >20 μM). Values in parentheses represent the 95% confidence interval. Addition of proguanil did not restore sensitivity to the D10_yeast DHODH cell line (EC_{50} >20 μM; data not shown).

(−CH_2OH (**98**, **99**) or −CH_2CH_2OH (**101**)). Addition of an amine functionality into the R at C2 (**74**−**84**, **89**−**97**) led to complete loss in inhibitory activity independent of the substitution pattern on the N atom or its position in the chain, thus confirming the lipophilic character of the channel. Transformation of C2 into a carbonyl moiety (**85** and **86**) also led to complete loss in inhibitory activity.

The most potent inhibitory activity against *Pf*DHODH was from compounds that contained an unbranched haloalkyl R group at C2, including −CF_2CH_3 (**35**−**38**), −$CF_2CH_2CH_3$ (**39**−**42**), or −CF_3 (**43** and **44**), an unbranched alkyl sulfur or oxygen containing group like −SCH_3 (**58**−**61**), or −SO_2CH_3 (**62**−**65**). Of these compounds, **37** (4-CF_3-aniline), **60** (4-CF_3-aniline), and **38** (4-SF_5-aniline), demonstrated the best potency against the parasite in whole cell assays (EC_{50}s below 20 nM against *P. falciparum* 3D7). For **35**−**38**, the addition of CF_2CH_3 to the C2 position improved activity by 4−40-fold against *Pf*DHODH and of 25−240-fold against the parasite compared to the matched analogues (**2**−**6**) containing a hydrogen at C2 (Figure 2). A similar improvement in potency was observed for addition of SCH_3 at C2 (**60**). Compounds containing 4-Cl (**35**, **39**) or 3-Cl (**36**, **40**) aniline showed greater fold improvement in potency against *Pf*DHODH than the 4-CF_3 (**37**) and 4-SF_5 (**38**) anilines, but the larger fold improvement has its origin in the poorer activity of the parent chloro compounds (R = H, **5** and **6**), and the absolute potency of these compounds against *Pf*DHODH is similar to those with 4-CF_3 and 4-SF_5 aniline.

Compounds **37** and **38** were also tested for whole cell activity in media supplemented with Albumax instead of human serum because we previously observed these two media gave different results for compounds containing the 4-SF_5 aniline.[19] As observed for compound **3**, compound **38** also showed 6−7-fold better activity against parasites cultured in media supplemented with Albumax in comparison to human serum, whereas for **37**, results were similar in the two media (Table 1).

Physicochemical Properties and Plasma Protein Binding. A selection of compounds were chosen for analysis of their

Table 2. Physicochemical Properties and in Vitro Metabolism[a]

compd	log $D_{pH\ 7.4}$	aqueous solubility pH 6.5 (μM)	human plasma protein binding[b] (%)	CL_{int} human/mouse (μL/min/mg protein)	E_h[c] human/mouse
2	2.5	21−43	86.9[b]	8/ND	0.29/ND
3	3.0	71−142	95.4[b]	<5/<6	0.20/0.20
6	2.4	ND	ND	38.2/ND	0.68/ND
11	2.8	170−350	86.1[b]	12.8/63.1	0.42/0.73
12	2.8	170−350	86.7[b]	78.3/125.4	0.81/0.85
13	3.0	39−78	87.5[b]	<5/14.4	<0.2/0.39
14	3.3	34−66	96.4[b]	<5/16.7	<0.2/0.42
15	3.2	83−170	84.9[b]	14.1/157.7	0.44/0.87
29	3.3	38−75	92.8[b]	<5/8.6	<0.2/0.27
30	3.5	16−32	97.7[b]	<5/12.6	<0.2/0.36
35	3.0	77−150	87.9[b]	16/62.8	0.47/0.73
36	3.0	77−150	88.2[b]	44.4/72.2	0.71/0.76
37	3.3	70−140	90.4[b]; 98.8[c]	<5/10.1	<0.2/0.31
38	3.6	30−60	97.4[b]; 99.9[c]	<5/8.1	<0.2/0.26
41	3.6	17−34	93.2 [b]	<5/6.5	<0.2/0.22
42	3.9	15−30	97.7 [b]	<5/6.7	<0.2/0.23
43	ND	ND	ND	<5/<6	<0.2/<0.2
44	3.7	30−60	ND	<5/<6	<0.2/<0.2
50	2.5	150−300	75.6 [b]	6.7/13.3	0.27/0.37
51	2.8	63−130	91.7 [b]	5.6/14.3	0.24/0.38
54	2.7	71−140	73.7 [b]	9.0/14.3	0.34/0.38
55	3.0	31−62	87.7 [b]	11.5/14.1	0.39/0.38
60	3.2	19−38	91.8 [b]	18.7/76.9	0.51/0.77
61	3.5	7.8−15	97.7 [b]	22.4/107.5	0.56/0.82
70	3.1	19−37	92.4 [b]	7.0/14.4	0.28/0.38
71	3.4	4−8	97.7 [b]	<5/11.3	<0.2/0.33
101	2.2	19−37	67.0 [b]	<5/6.9	<0.2/0.23

[a] Data for **2**, **3**, and **6** were previously reported.[16,19] [b] Chromatographic method. [c] Ultracentriguation method. E_h < 0.3 represents low predicted metabolism, E_h 0.4−0.7 moderate predicted metabolism, and E_h >0.8 high predicted metabolism. ND, not determined.

physicochemical properties including log *D*, aqueous solubility, and plasma protein binding (Table 2). The compounds in the series all have physicochemical properties that are consistent with good oral absorption (MW <430, H bond donors <2, and H bond acceptors <6, polar surface area <90 Å^2). The log *D* for the series of compounds was found to range from 2.8 to 3.9 and was typically highest for compounds containing a 4-SF_5 aniline. Aqueous solubility varied from poor to good, and compounds with 4-SF_5 aniline were the least soluble while those with 3- or 4-Cl aniline were among the best. The most potent compounds (**37** and **38**) showed mid range solubility and, again, the 4-SF_5 aniline (30−60 μM) derivative was less soluble than the 4-CF_3 aniline (70−140 μM). Human plasma protein binding was evaluated by two methods: (1) a chromatographic method that allowed rapid evaluation of a larger number of compounds and was useful for comparative purposes, and (2) a more rigorous ultracentrifugation method that provided an accurate absolute value for assessing total versus free drug concentrations in the in vivo models. Using the chromatographic method, compounds in the series typically ranged from 85 to 98% protein bound, with those containing the 4-SF_5 aniline having both the highest log *D* and the highest plasma protein binding. For those compounds (**37** and **38**) that were evaluated with both methods, the ultracentrifugation method yielded a higher protein binding value than the chromatographic method. Protein binding for **38** was found to be very high in both human and mouse plasma (99.9 and 99.6%, respectively), whereas the binding of **37** was somewhat lower (98.8 and 97.4%, respectively). For both **37** and **38**, protein binding in rat plasma (94.2 and 97.3%, respectively) was lower than that in either mouse or human plasma, but the binding of **38** was still higher than that of **37**. Protein binding in the Albumax media used for in vitro activity assessment was not measured but it is likely that the intrinsic "free" in vitro potency of compound **38** is extremely high.

In Vitro Metabolic Stability. As an initial screen for good in vivo pharmacokinetic properties, metabolic stability was evaluated in vitro using human and mouse hepatic microsomes. We have previously observed a good correlation between stability in microsomal assays and exposure in rodents for the triazolopyrimidine series.[16,19] In this assay, in vitro intrinsic clearance (CL_{int}) values were measured and used to predict an in vivo intrinsic clearance and, subsequently, an in vivo hepatic extraction ratio (E_h) (fraction of compound predicted to be metabolized on the first pass through the liver) with the assumption that hepatic metabolism would represent the primary clearance mechanism. Compounds that contained $-CF_2CH_3$ (**37**−**38**), $-CF_2CH_2CH_3$ (**41**−**42**), or $-CF_3$ (**43**−**44**) at the C2 position showed low intrinsic clearance (CL_{int} <6 μL/min/mg microsomal protein in human microsomes and <10 μL/min/mg in mouse microsomes) in these

assays, provided that these C2 R groups were coupled with the 4-CF_3 (**37**, **41**, **43**) or 4-SF_5 (**38**, **42**, **44**) aniline (Table 2). The low intrinsic clearance values suggested that these compounds would exhibit good metabolic stability in both mice and humans. Compounds containing 4-Cl (**11**, **35**) or 3-Cl (**12**, **36**) aniline had much higher intrinsic clearance values, suggesting that they would be more rapidly metabolized in vivo. Compounds containing an $-CH_2CH_3$ (**13** and **14**), an $-OCH_2CH_3$ (**70** and **71**), −cyclopropyl (**29** and **30**), $-CH_2OCH_3$ (**50** and **51**), $-CH_2CH_2OCH_3$ (**54** and **55**), or $-CH_2CH_2OH$ (**101**) at C2 also showed good metabolic stability, again provided that these C2 R groups were coupled to either 4-CF_3 or 4-SF_5 rather than to 3- or 4-Cl aniline. However, these compounds were all less potent than those containing a haloalkyl (**37** and **38**) group. Compounds that contained sulfur (**60** and **61**) were among the most potent *Pf*DHODH inhibitors in the series, however they showed poor metabolic stability and were therefore not likely to show sufficient exposure in vivo to provide efficacy. Thus, the compounds that provided the best balance between potency and metabolic stability were identified to be **37** and **38**, and these were selected as the front-runners for further characterization.

Species Selectivity and Evaluation of Cytotoxicity. Select compounds were evaluated for activity against *P. berghei*, *P. vivax*, and human DHODH (Table 1). The addition of groups larger than hydrogen at C2 systematically reduced binding affinity to the *P. berghei* enzyme; for example, **37** and **38** were 100-fold less potent on *P. berghei* DHODH than on the *P. falciparum* enzyme. In contrast to the results on *Pb*DHODH, *P. vivax* DHODH was inhibited with similar potency to *Pf*DHODH by both **37** and **38** (*P. vivax* DHODH IC_{50} = 0.084 and 0.073 μM, respectively), suggesting that both compounds will have good activity against *P. vivax* parasites. Compounds in the series continued to show excellent selectivity against the human enzyme, and the IC_{50} for *h*DHODH was >100 μM (Table 1) for all of the evaluated compounds, with the exception of **44**, which showed weak activity against the human enzyme (IC_{50} = 41 μM).

The two front-runner compounds **37** and **38** were tested against an expanded panel of *P. falciparum* strains (Table 3). Both compounds showed similar potency against drug-sensitive and drug-resistant (chloroquine and atovaquone) strains. Cytotoxicity was assessed against both a mouse (L1210) and human (HepG2) cell line, and no activity within the tested range (up to 50 μM) was observed for either compound against these cell lines.

Evaluation of the Antimalarial Mode of Action. To confirm that cell killing by the DHODH inhibitors results from inhibition of *Pf*DHODH, we tested the inhibitors against a *P. falciparum* D10 cell line transfected with cytoplasmic yeast DHODH (D10_yDHODH) that uses fumarate instead of mitochondrial CoQ as the final electron acceptor.[26] This cell line has previously been demonstrated to rescue parasites from the toxicity of both mitochondrial bc1 complex inhibitors such as atovaquone[26] and *Pf*DHODH inhibitors such as our triazolopyrimidines.[13,27] Addition of proguanil has been shown to restore sensitivity of D10_yDHODH to bc1 complex inhibitors but not to specific *Pf*DHODH inhibitors. The D10_yDHODH cell line is resistant to both **37** and **38**, and this result was independent of the presence of proguanil in the culture media, demonstrating that the antimalarial effect of these compounds is due to inhibition of *Pf*DHODH. Representative data for **38** are shown in Figure 2.

X-Ray Structure Determination of PfDHODH in Complex with 37. The X-ray structure of *Pf*DHODH in complex with **37** was solved to 2.95 Å resolution (Supporting Information Table S1, Figure S1). Both the triazolopyrimidine ring and the aniline ring superimpose closely onto the position of **2** (pdb 3I6R),[22] although there is a slight shift of both rings away from FMN and toward Phe188 (rmsd = 0.4 Å) (Figure 3A). The key interactions are preserved, including an H-bond between His185 and the pendant nitrogen that bridges between the triazolopyrimidine ring and the phenyl ring and an H-bond between Arg265 and the pyrimidine nitrogen N4. The CF_2CH_3 R-substituent of **37** binds into the channel that extends from the triazolopyrimidine ring toward the FMN and makes good van der Waals interactions throughout the pocket, which is composed of Ile263, Ile272, the hydrophobic portion of the Arg265 side chain, and of the hydroxyl and ring of Tyr528 (Figure 3B). Thus the addition of the $-CF_2CH_3$ R-substituent to the scaffold provides key hydrophobic interactions with the enzyme in the one significant space that was left unoccupied by the previous analogues from the series. Furthermore, the electron withdrawing effect of the fluorine atoms will reduce electron density on the nitrogens within the 5-membered triazole ring. This may, therefore, contribute to the potency increase as a result of decreased desolvation. These observations provide a structural explanation for the improved potency of these analogues. The structure also provides insight as to why R groups that are larger than propyl are inactive (e.g., **19**−**22**), as the pocket has insufficient room to accommodate a branched chain functionality as large as *iso*-butyl. The complete inactivity of R groups containing an amine functionality is explained by the hydrophobicity of the R-pocket and the lack of H-bonding partners in the R-pocket except for lone pair electrons of the Tyr528 side chain hydroxyl. Finally, the X-ray structure provides insight into the poor binding of **37** to *Pb*DHODH. The replacement of Gly181 with Ser in *Pb*DHODH may lead to a restriction in the size of the R-group that can be accommodated by this enzyme.

Table 3. Comparison of *P. falciparum* Cell Lines and Mammalian Cytotoxicity Data[a]

compd	**38** EC_{50} (μM)	**37** EC_{50} (μM)
P. falciparum 3D7 (μM)	0.043 (0.034−0.055)	0.013 (0.012−0.014)
P. falciparum D6 (μM)	0.022 (0.014−0.034)	0.012 (0.011−0.013)
P. falciparum K1 (μM)	0.057 (0.048−0.068)	0.016 (0.014−0.017)
P. falciparum HB3 (μM)	0.027 (23−31)	0.0079 (0.0072−0.0086)
P. falciparum Dd2 (μM)	0.057 (0.041−0.079)	0.013 (0.012−0.014)
P. falciparum TM90C2B	0.015 (0.013−0.018)	0.0046 (0.0013−0.016)
P. falciparum TM90C2A	0.031 (0.023−0.033)	0.0079 (0.0076−0.0081)
mouse L1210	>50	>50
human Hep G2 (μM)	>50	>50

[a] Additional *P. falciparum* strains that were tested include drug sensitive strains (D6, HB3, and NF54), chloroquine resistant strains (Dd2) chloroquine and pyrimethamine resistant (K1), and atovoquone resistant strains (TM90C2B and TM90C2A). Data were collect on strain 3D7 as a comparator. Data were collected in triplicate and values in parentheses represent the 95% confidence interval. Data were collected using human serum containing media.

Pharmacokinetic Properties in Mice and Rats. To further assess the potential for **37** and **38** to be selected as clinical development candidates, their pharmacokinetic properties were assessed in mice and rats. In noninfected mice, **37** and **38** showed good exposure following single dose oral administration (Figure 4 and Table 4B). Maximum plasma concentrations (C_{max}) and

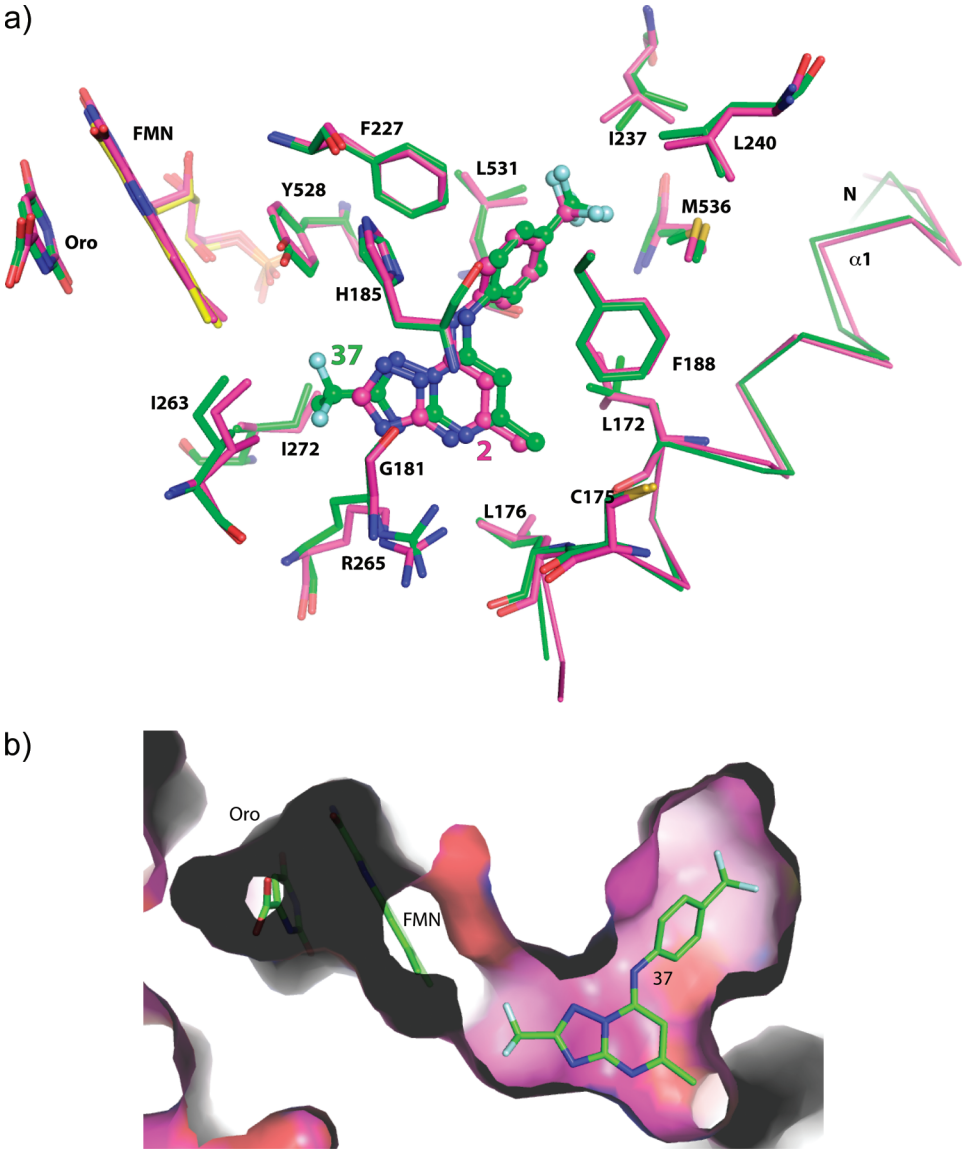

Figure 3. X-ray structure determination of *Pf*DHODH in complex with **37**. (a) Structural alignment of *Pf*DHODH$_{\Delta 384-413}$−**37** (green) in comparison to *Pf*DHODH bound with **2** (PDB 3I6R) (pink). Residues within 4 Å of the bound inhibitor are displayed. L-Orotate and the FMN cofactor are also displayed. (b) van der Waals surface representation of *Pf*DHODH bound with **37**. The enzyme surface is shown in pink, and orotate, FMN, and **37** are shown in green as sticks. Structures were displayed using PyMol.

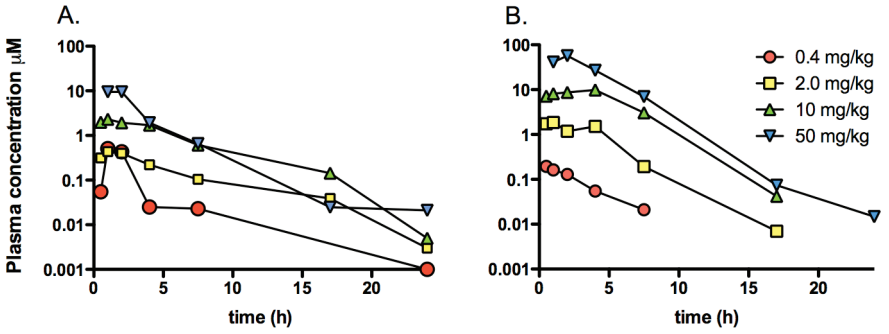

Figure 4. Pharmacokinetic analysis of (A) **38** and (B) **37** after oral dosing in mice (n = 1 mouse per time point). Plots represent plasma concentration versus time after a single dose. Dose levels and route are shown in the graph legend.

AUC_{0-inf} values of **38** increased approximately in proportion to the increase in dose over the range 0.4−10 mg/kg range, however the relative increase was somewhat reduced at 50 mg/kg dose. Compound **37** exhibited dose proportional increases in

dx.doi.org/10.1021/jm200592f |*J. Med. Chem.* 2011, 54, 5540–5561

Table 4. In Vivo Pharmacokinetic Data for Key Triazolopyrimidines in Mice[a]

(A) compounds **37** and **38** evaluated after a single oral dose of 0.4, 2, 10, or 50 mg/kg

parameter	37	38
po dose (mg/kg)	0.4, 2, 10, 50	0.4, 2, 10[b], 50
$t_{1/2}$ (h)	2.1, 1.9, 1.6, cnc	4.1, 3.5, 2.5, 3.2
C_{max} (μM)	0.20, 1.85, 9.86, 57	0.06, 0.44, 3.1, 9.53
T_{max} (h)	0.5, 1, 4, 2	0.5, 1.0, 1.5, 2.0
time $T_{C>1\ \mu M}$ (h)	0, 6, 14, 14	0, 0, 8, 6
plasma AUC_{0-inf} (μM·min)	40, 569, 4207, 14815[c]	27, 163, 1357, 2028
plasma protein binding (%)	97.4	99.6

(B) compounds **13**, **41**, **70**, and **71** after a single oral dose of 10 or 20 mg/kg

parameter	13	41	70	71
po dose (mg/kg)	20	10	20	20
$t_{1/2}$ (h)	8.4	3.1	1.4	2.7
C_{max} (μM)	12.6	3.5	5.8	1.1
T_{max} (min)	60	30	60	60
time $T_{C>1\ \mu M}$ (h)	5	4	6	3
AUC_{0-inf} (μM·min)	1624	652	1241	608

[a] cnc, could not calculate. [b] Values at 10 mg/kg are the average for 2 independent experiments. [c] $AUC_{0-48\ h}$.

C_{max} and AUC_{0-inf} across the full dose range (0.4−50 mg/kg). Four other compounds (**13**, **41**, **70**, and **71**) with good potency (EC_{50} < 0.1 μM) against the parasite and good metabolic stability were also tested to evaluate plasma exposure in mice (Table 4B). Compounds **13** and **70** showed similar exposure to **37** and **38** as evaluated by both C_{max} and AUC_{0-inf}, while compounds **41** and **71** had somewhat lower exposure.

The pharmacokinetic properties of **37** and **38** in rats were examined after both intravenous (iv) and oral (po) administration (Table 5 and Figure 5). After iv dosing, **38** had low clearance (4−6 mL/min/kg), moderately high volume of distribution (3−6 L/kg), and a long half-life (10−13 h), whereas **37** exhibited higher clearance (13−23 mL/min/kg), similar volume of distribution (3 L/kg), and a shorter half-life (4−6 h). Neither compound was excreted unchanged in urine. After oral dosing, both **37** and **38** demonstrated good oral bioavailability and long half-lives (Table 5 and Figure 5), however the increase in both the time to reach the maximum concentration (T_{max}) and the half-life with increasing dose suggested a slower rate of absorption with increasing dose. Compound **38** showed dose-proportional kinetics over the oral dose range of 2−50 mg/kg, while for **37**, there was evidence for dose-dependency over the range of 2−20 mg/kg.

In Vivo Efficacy of 37 and 38 in the *P. falciparum* SCID Mouse Model. The observation of good bioavailability of **37** and **38** in mice and rats led us to test these compounds in an in vivo efficacy model. The poor activity of **37** and **38** against *Pb*DHODH prohibited the use of the *P. berghei* mouse model to evaluate their in vivo efficacy. To overcome this issue, **37** and **38** were tested against the human malaria parasite *P. falciparum* in the humanized SCID mouse model.[28] To provide a direct comparator to our prior studies that used the *P. berghei* mouse model, compound **4** (in vivo mouse *P. berghei* ED_{50} = 10 mg/kg for **4**)[19] was included in the SCID mouse study. Unlike **37** and **38**, **4** has similar activity against *Pf*DHODH and *Pb*DHODH, and thus was able to be evaluated in both the SCID mouse and the *P. berghei* mouse models. Chloroquine was also included as a control to represent a standard antimalarial agent with known behavior in the SCID mouse model.

Table 5. In Vivo Pharmacokinetic Properties for 37 and 38 in Rats (Average of *n* = 2 per Dose Level)

parameter	37	38
iv dose (mg/kg)	1; 4.5	0.9; 2.6
clearance (mL/min/kg)	23.2; 12.6	3.6; 6
$t_{1/2}$ (h)	6.1; 3.8	10.1; 12.6
volume of distribution (L/kg)	3.3; 2.9	2.9; 5.9
po dose (mg/kg)	2.0 ; 21.2	2.1; 18.8; 46.7
T_{max} (min)	60; 195	195; 420; 1020
C_{max} (μM)	0.9; 11.4	0.75; 3.9; 6.4
bioavailability (*F*%)	97; >100	66; 57; 61
$t_{1/2}$ (h)	6; 17	11.6; 15.5; 27.9
AUC_{0-inf} (μM·min)	233; 20492	929; 7292; 19305
blood:plasma	0.7 − 0.8	0.7 − 0.8
plasma protein binding (%)	94.2	97.3

Compounds (**4**, **37**, and **38**) were dosed orally 1× daily for 4 days beginning 3 days after mice were infected with parasites. The ED_{50}s were determined 24 h after the final dose as described.[28] Both **37** and **38** markedly inhibited parasitemia in peripheral blood of mice (ED_{90} = 25.9 and 8.1 mg/kg, respectively), with **38** showing efficacy at doses in the order of chloroquine (ED_{90} = 4.9 ± 0.5 mg/kg) and artesunate (12.7 ± 1.3 mg/kg)[28] (Table 6 and Figure 6). Compound **38** has a clear potency advantage over **37**, however both were more potent than **4** (by 7-fold and 2-fold respectively) and both meet our development criteria for a preclinical candidate (defined as an ED_{90} < 30 mg/kg in this model). Interestingly, aberrant late trophozoites/early schizonts were detected in peripheral blood of mice treated effectively with compounds **37** and **38**, which is consistent with a mechanism of action affecting parasite metabolism. The comparator compound **4** showed similar efficacy in the SCID model (ED_{50} = 19 mg/kg) to what was observed previously in the *P. berghei* model (ED_{50} = 10 mg/kg).[19]

A pharmacokinetic study in uninfected and infected SCID mice engrafted with human erythrocytes was performed in order to interpret the efficacy results. The oral exposure of **4**, **37**, and **38** upon po administration at 10 mg/kg indicated that infection did not significantly change compound disposition of compounds (Table 6). Interestingly, the overall exposure in whole blood for the three compounds studied was similar, which suggest that differences in intrinsic potency rather than changes in pharmacokinetic parameters are most likely responsible for the differences in efficacy detected in vivo.

DISCUSSION

The burden of malaria falls disproportionately on the world's poorest countries and, while effective treatments are in place, the continual challenge is to stay ahead of the parasite's unyielding ability to select for drug resistance. The identification of new chemical classes with different modes of action than existing drugs and which also show good drug-like properties and efficacy against the parasite is the key to treatment of the disease. Through a structure-guided lead optimization program that

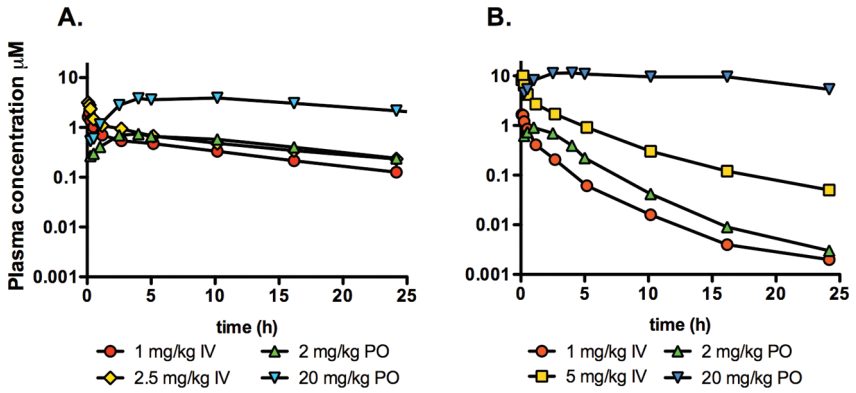

Figure 5. Pharmacokinetic analysis of (A) **38** and (B) **37** after oral (po) or iv dosing in rats (n = 2 rats per dose route). Plots represent plasma concentration versus time after a single dose. Dose levels and route are shown in the graph legend.

Table 6. In Vivo Efficacy and Pharmacokinetic Properties in the SCID Mouse *P. falciparum* Model after Oral Dosing (Average of n = 3 Mice Per Compound)[a]

	4	37	38
ED_{50}/ED_{90} (mg/kg)	19/59	9.6/26	2.8/8.1
po dose (mg/kg)	10	5.7	7.0
blood $AUC_{(0-t)\#}$ uninfected/infected (μM·min)	3848/3173	2521/2740	3469/3427
C_{max} uninfected/infected (μM)	8.5/8.2	6.3/6.3	6.1/5.3
T_{max} uninfected/infected (h)	2.0/3.3	2.7/1.7	4/6.7

[a] ED_{50} for chloroquine control 3.2 mg/kg. [#] t = 10 h after dosing for **4** and **37** and 24 h after dosing for **38**. This time point represents the last time point where compounds were detectable in whole blood of animals.

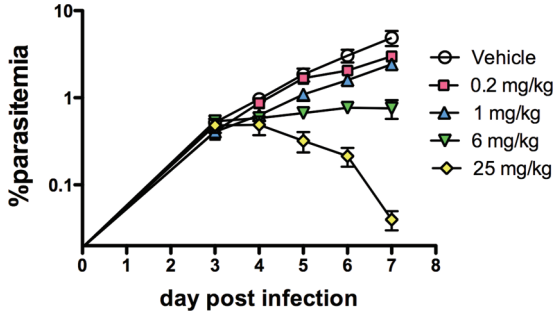

Figure 6. Efficacy of **38** in SCID mice infected with *P. falciparum* after oral dosing. Mice were infected with parasites on day zero and a single oral dose/day was given on days 3, 4, 5, and 6. The limit of detection of the assay is 0.01% parasitemia. Dose levels are shown in the graph legend.

integrated pharmacokinetic and metabolism assessment into the medicinal chemistry plan, we have identified two potent *Pf*DHODH inhibitors (**37** and **38**) from the triazolopyrimidine series that meet previously established progression criteria. The antiparasitic activity of these compounds in the humanized SCID mouse *P. falciparum* model (ED_{90} < 30 mg/kg) suggests that both compounds show good in vivo efficacy. Parallel pharmacokinetic studies in mice and rats demonstrated sustained plasma concentrations after oral dosing consistent with once daily dosing, and both compounds are active against drug sensitive and drug resistant strains of the parasite, all of which are necessary to meet the target product profile.[11] These compounds represent a significant breakthrough in potency compared to previously identified compounds from this series, and they represent the first that are potent enough to be progressed for clinical development.

The triazolopyrimidines were identified early in our program to develop *Pf*DHODH inhibitors for the treatment of malaria, however previous compounds from the series have either lacked metabolic stability (**1**) or have shown insufficient potency against the parasite (**2**−**4**).[16,17,19] The X-ray structure of **1** and **2** bound to *Pf*DHODH showed that a narrow channel leading from the C2 position of the triazolopyrimidine ring toward the FMN cofactor afforded the best chance to build additional functionality into the molecule to improve potency.[22] We have systematically evaluated a series of alkyl, haloalkyl, ether, and amine substituents in this position, leading to the identification of several functional groups that provided the desired boost in potency. Most of the best functional groups at C2 are electron withdrawing and hydrophobic, and the rank order of potency against both the enzyme and the parasite in whole cell assays was $-CF_2CH_3$, $-SCH_3 > -CF_3$, $-CF_2CH_2CH_3 > -OCH_2CH_2 > -CH_2CH_3$. Larger substituents and branched chain or cyclic groups were less active. These results match well with the observation from the X-ray structure of **37** bound to *Pf*DHODH, which shows that the C2 binding pocket is narrow and dominated by hydrophobic residues. As was observed in prior compounds that contain hydrogen at the C2 position,[19] anilines substituted with 4-CF_3 or 4-SF_5 provided the best balance between potency and good metabolic stability. Compounds with 4-Cl or 3-Cl showed somewhat lower potency and were notably less metabolically stable.

In contrast to the good activity of the haloalkyl substituents, all compounds containing amines at C2 were inactive. The X-ray structure analysis shows that except for the hydroxyl oxygen of Tyr528, there are no H bond acceptors in the pocket that would bind a C2 substituent. In the absence of a major ligand induced reorganization of the pocket, the Tyr528 side chain oxygen is geometrically inaccessible to any potential hydrogen bonding group such as an amine directly linked through a tetrahedral carbon attached to the triazolopyrimidine at C2. The addition of alcohols at C2 also led to reduced activity. These compounds (particularly $-CH_2CH_2OH$ at C2) were designed to displace the bound water molecule (W15) observed to bind between the

dx.doi.org/10.1021/jm200592f |*J. Med. Chem.* 2011, 54, 5540–5561

Tyr528 hydroxyl and N3 on the triazolopyrimidine in the X-ray structure of *Pf*DHODH bound to **1**[22] and to test the hypothesis that the resulting gain in entropy would improve binding affinity. However, compounds with $-CH_2OH$ (**98** and **99**) and $-CH_2CH_2OH$ (**101**) at C2 were less active then the parent compounds **2**, **5**, and **6**, suggesting that even if the bound water was displaced, this mechanism did not provide additional binding energy possibly owing to the energetic cost of desolvating the hydroxyl of **101** upon binding to *Pf*DHODH.

The most potent of the analogues with $-CF_2CH_3$ at C2 (**37** and **38**) were identified as the front-runners and evaluated in a series of additional assays to determine their development potential. These compounds showed 25−50-fold better activity against *P. falciparum* 3D7 cells in whole cell assays than that of compounds containing hydrogen at C2. This improvement in potency was achieved while remaining on target, as parasites transfected with yeast DHODH were resistant to both inhibitors as would be expected if the cell killing occurred via DHODH inhibition. Both compounds also showed good activity against *Pv*DHODH, suggesting that they will also be useful to treat *P. vivax* infections, and both were fully active against drug resistant strains of the parasite, including atovaquone and chloroquine resistant strains.

Compounds **37** and **38** exhibited good metabolic stability when evaluated in hepatic microsomal assays, and pharmacokinetic profiles confirmed low clearance and good oral bioavailability in both mice and rats leading to high and extended plasma exposure profiles. In rats, compound **37** showed significant dose dependency in the kinetic profile even over a relatively low dose range. The greater than proportional increase in AUC_{0-inf} for **37**, and the corresponding apparent bioavailability of >100% at the higher dose, suggested saturation of the clearance pathway(s) with increasing dose for this compound. In comparison, **38** exhibited reasonably dose proportional kinetics in rats over a broad dose range. The delay in T_{max} and prolongation of the half-life with increasing dose for both **37** and **38** suggests a dose-dependent reduction in the rate of absorption, possibly due to dissolution rate-limited absorption resulting from the relatively low aqueous solubility (Table 2). Importantly, the low solubility did not appear to limit the extent of absorption based on the high bioavailability for both compounds.

Compounds **37** and **38** required a significantly lower dose to clear parasites in a SCID mouse model than prior compounds from the triazolopyrimidine series, and this finding can be attributed to the combination of the significantly improved potency and the good plasma exposure profile. For **38**, the dose required (ED_{50}/ED_{90} 2.8/8.1 mg/kg) was similar to that for chloroquine examined in the same study, and these values were 7-fold lower than for the previous most efficacious compound from the series (**4**) when tested in the same SCID mouse model. The matched analogue of **38** containing a hydrogen at C2 (**3**) has not been tested in this model. However, because **3** and **4** have similar activity against *Pb*DHODH and *Pf*DHODH, they were both previously tested for efficacy in the *P. berghei* mouse model.[19] In this experiment the ED_{50} for **3** was 2-fold higher than that for **4**, suggesting that the addition of the CF_2CH_3 group to C2 may have improved in vivo efficacy by up to 14-fold (e.g., **38** was 7-fold more potent than **4** in the SCID model, and **4** is 2-fold more potent than **3** in the *P. berghei* model). These data also differentiate these compounds from the reported *N*-alkyl-5-(1*H*-benzimidazol-1-yl)thiophene-2-carboxamides where the ED_{50} in the *P. berghei* in vivo model for the most potent of these compounds (Genz-667348) was 2−6-fold higher (depending on the parasite strain) and required BID dosing,[21] in comparison to the results obtained for **38** where QD dosing was used.

Results for the plasma protein binding studies with **37** and **38** indicate that the binding of **38** was higher than that of **37** in each of the species tested (e.g., human, rat and mouse), meaning that the free fraction of **38** would be lower than that of **37**. While binding in the Albumax media used for the in vitro cell-based assay has not been assessed, the plasma protein binding trends would suggest that **38** would also exhibit higher binding, and lower free concentrations, in the Albumax media. Because **37** and **38** had similar activity in the *P. falciparum* cell-based assay, a lower free fraction for **38** may indicate that it is actually more potent than **37** if the free concentrations are considered. This hypothesis, combined with the longer half-life and more extended exposure profile for **38** measured in normal mice, may explain the difference in potency for the two compounds in the SCID mouse model despite their similar measured whole blood concentrations.

On the basis of the better in vivo efficacy and the observation of more linear pharmacokinetics in rats, **38** has been chosen as the lead compound for further workup toward clinical candidate status. While none of the other compounds with potency in the same range as **37** and **38** (EC_{50} < 20 nM in the whole cell *P. falciparum* assay) were metabolically stable, compounds **13** and **70** were the next best compounds with respect to the combination of potency and metabolic stability. Both compounds also showed good exposure after oral dosing in non-infected mice and thus might serve as backup compounds to the identified front-runner (**38**).

CONCLUSION

We have identified a compound (**38**) from the triazolopyrimidine series of *Pf*DHODH inhibitors that meets development criteria, showing efficacy against *P. falciparum* in vivo in a murine model, activity against drug resistant parasite strains, and activity against *Pv*DHODH. Importantly, the excellent in vivo efficacy was obtained with QD dosing, attributable to the long half-life and excellent oral exposure, and suggesting that **38** will be able to meet the target product profile of cure in three consecutive daily doses in patients. Final validation of the development potential of **38** will require toxicological studies in animals and the successful clinical proof of concept of a DHODH inhibitor for the treatment of malaria in man.

MATERIALS AND METHODS

Determination of Enzyme Inhibition Constants. The plasmids used for the *E. coli* expression of His-tagged *Pf*DHODH, *Pb*DHODH, and *h*DHODH have been previously described.[16−18] The *P. vivax* DHODH expression construct was generated as follows. A 1266-bp DNA fragment of *Pv*DHODH was amplified by PCR from genomic *P. vivax* strain Belem DNA provided by John Barnwell (CDC) using primers 5′- GTA GTA GCT CTA **TAC** ATG TAT TTC GAG TCC TAC GAC CCC G-3′ and 5′-CTC GAG GGC GGC CCG CCG GTG GGC CCG CCC GAC GGC GT-3′ and ligated into Zero Blunt TOPO vector (Invitrogen). QuickChange site-directed mutagenesis kit (Stratagene) was used to remove an internal *NdeI* site from *Pv*DHODH using primers 5′-TGT CTA CTC ACA TGA TTT CTC AAA TG-3′and 5′-CAT TTG AGA AAT CAT GTG AGT AGA CA-3′. The resultant clone was used to PCR amplify the *Pv*DHODH region introducing *XhoI* and *NdeI* restriction sites, respectively, with primers 5′-TGG AAT TCG

CCC TCG AGG GCG GCC CGC CGG-3′ and 5′-GTA GTA GCT CTA CAT ATG TAT TTC GAG TCC TAC GAC-3′. This PCR product was ligated into Zero Blunt TOPO vector (Invitrogen) and digested with *XhoI* and *NdeI* to excise the DHODH coding sequence, which was then ligated to pET22b expression vector (Novagen) to generate the C-terminal 6xHis-tagged truncated *Pv*DHODH construct used for recombinant protein expression. All four proteins were expressed as soluble truncated proteins in the absence of the N-terminal domain that includes the membrane-spanning region of the protein. Proteins were purified as previously described by Ni^{2+}-agarose chromatography and gel filtration.[17,18]

Steady-state kinetic assays to determine the IC_{50}s for inhibitors were performed as previously described.[17,18] Briefly, a dye-based assay that couples the final oxidation of CoQ to the reduction of 2,6-dichloroindophenol (DCIP) was followed at 600 nm (ε = 18.8 mM^{-1} cm^{-1}). Enzyme stocks were diluted into assay buffer containing 0.1 mM BSA to make a 100× working stock solution, which was kept on ice. Assays were initiated by adding 5 μL of this stock solution to 500 μL of assay buffer containing substrates and inhibitors. Conditions were as follows: DHODH (E_T = 5−10 nM), substrates (0.2 mM L-dihydroorotate and 0.02 mM CoQ_D), DCIP (0.12 mM), and assay buffer (100 mM HEPES, pH 8.0, 150 mM NaCl, 10% glycerol, 0.1% Triton) at 20 °C. Inhibitor concentration was varied in a 3-fold dilution series (0.01−100 uM). The percent inhibition relative to the no inhibitor control was determined (v_i/v_o × 100), and data were fitted to the log[I] vs response (three parameters) equation in Graph Pad Prism to determine the IC_{50}.

X-Ray Structure Determination of $PfDHODH_{\Delta 384-413}$−37. *Protein Purification.* Protein for crystallization was expressed from a different construct than that used for the inhibition studies. Deletion of a surface loop (Δ384−413) was necessary to generate a protein that could be crystallized, and both the construct and the purification procedure have been previously described.[21,22] These prior studies also showed that deletion of this loop had no effect on enzyme activity. Preliminary crystallization conditions were found using the random crystallization screen *AmSO4* suite (Nextal). The initial conditions were refined by variation of pH, precipitant, and protein concentrations to find optimal conditions. Crystallizations were set up using the hanging drop vapor diffusion method at 20 °C. Crystals of *Pf*$DHODH_{\Delta 384-413}$−**37** complex were obtained by mixing reservoir solution (1.64−1.74 M ammonium sulfate, 0.1 M sodium acetate, pH 4.1, and 10 mM DTT) with an equal volume of *Pf*$DHODH_{\Delta 384-413}$ (20 mg/mL) pre-equilibrated with 0.5 mM **37** and 2 mM dihydroorotate. Crystals typically grew in 4−7 days.

Diffraction data were collected at 100K on beamline 19ID at Advanced Photon Source (APS) using an ADSC Q315 detector. The crystal of *Pf*$DHODH_{\Delta 384-413}$−**37** diffracted to 2.95 Å and has a space group of $P6_4$ with the cell dimension of $a = b$ = 86.6, c = 138.2. The structure contains only one molecule of *Pf*DHODH in the asymmetric unit. Diffraction data were integrated and intensities were scaled with HKL2000 package.[29]

Crystallographic phases for *Pf*DHODH inhibitors were solved by molecular replacement with Phaser[30] using the previously reported structure of *Pf*$DHODH_{\Delta 384-413}$ (PDB ID 3I65[22]) with ligands removed as the search model. Structures were rebuilt with COOT,[31] refined with REFMAC[32] to R and R_{free} of 0.236 and 0.285, respectively (Table S2 and Figure S1, Supporting Information). The final structure contains residues 161−347, 355−383, and 414−565 and 5 water molecules. Electron density was not observed, for loop 348−354 is missing. All residues in the final structure were within the allowed section of the Ramachandran plot (Table S2, Supporting Information). Water molecules were added if the density was stronger than 3.4 σ and removed if the density was weaker than 1 σ in the density map with ARP/warp.[33]

Molecular Modeling. Structures were displayed using PyMol (DeLano Scientific LLC, San Carlos, CA). The rmsd between the structures of *Pf*DHODH bound to **37** versus **2** was calculated using DaliLite.[34]

In Vitro Assay of *P. falciparum*. Parasites were grown in Gibco-Invitrogen RPMI-1640 supplemented with 20% human type A+ plasma and 2% (w/v) red blood cells[35] or with Gibco-Invitrogen 0.5% Albumax I. Before transferring cultures to media with in Albumax, cells were washed three times in RPMI-1640 to remove plasma-supplemented medium. The D10 cell line containing yeast DHODH was cultured in the absence and in the presence of proguanil (5 μM). Low-passage L1210 mouse leukemia cells (American Type Culture Collection) were also grown in plasma-supplemented RPMI-1640, while HepG2 human hepatocarcinoma cells (American Type Culture Collection) were grown in F12/DMEM (1:1). Blood products were obtained from Biochemed Services, Virginia. [^{3}H]-hypoxanthine uptake was used to measure cell growth, and incorporation of no-drug samples was compared to drug-treated cells as described previously.[36] Data were fitted to the log[I] vs response − variable slope (four parameter) model in Graph Pad Prism to determine the ED_{50}'s for inhibition of parasite growth.

Physicochemical Properties. Partition coefficients (log $D_{pH\ 7.4}$) were estimated by comparing their chromatographic retention properties to a set of standard compounds with known partition coefficients. Data were collected using a Waters 2795 HPLC instrument with a Waters 2487 dual channel UV detector with a Phenomenex Synergi Hydro-RP 4 μm (30 mm × 2 mm) column. The mobile phase was aqueous buffer (50 mM ammonium acetate, pH 7.4) and acetonitrile with an acetonitrile gradient of 0−100% over 10 min. Compound elution was monitored at 220 and 254 nm.

Aqueous solubility was estimated by nephelometry. Compound in DMSO was spiked into either pH 6.5 phosphate buffer or 0.01 M HCl (approximately pH 2.0), with the final DMSO concentration being 1%. Samples were then analyzed by nephelometry to determine the solubility range as described previously.[37]

Plasma protein binding was assessed using two different methods: (1) chromatographic retention on a human albumin column, or (2) by ultracentrifugation. The chromatographic method utilized a human albumin column (ChromTech Chiral-HSA 50 mm × 3.0 mm, 5 μm, Sigma-Aldrich) and compared retention characteristics to a series of standard compounds with known human plasma protein binding values using a modification of a published method.[38] A Waters 2795 HPLC system equipped with a Waters 2487 dual channel UV detector (monitored at 220 and 254 nm) was used with a mobile phase comprised of aqueous buffer (25 mM ammonium acetate buffer pH 7.4) and 30% isopropyl alcohol in the same buffer. The isopropanol concentration was varied over a 10 min gradient, and the column was reconditioned prior to the next injection.

Measurement of plasma protein binding by ultracentrifugation was performed using human, rat, and mouse plasma. Human blood was obtained from the Australian Red Cross Blood Service, rat blood from male Sprague−Dawley rats, and mouse blood from male Swiss outbred mice. Plasma was separated from whole blood by centrifugation and stored frozen at −80 °C (human) or −20 °C (rat and mouse). Compound stock solutions were prepared in DMSO (1 mg/mL) and then further diluted in 50% (v/v) acetonitrile (20 and 200 μg/mL). Plasma at 37 °C was spiked with compound stock solutions to give concentrations of 200 and 2000 ng/mL (maximum final DMSO and acetonitrile concentrations were 0.2% and 0.5%, respectively), followed by equilibration at 37 °C for 1 h and ultracentrifugation (Beckman Rotor type 42.2 Ti; 223000g and 37 °C) for 4.2 h to separate plasma proteins from plasma−water. An aliquot of supernatant (i.e., plasma−water) was taken from each tube to determine free concentration. The total concentration was determined in noncentrifuged plasma samples similarly incubated. The concentration of test compound in samples was determined by LC-MS using calibration standards prepared in the respective matrices. The percentage of compound bound to plasma

proteins (% bound) was calculated according to the following equation: %bound = $100(C_{plasma} - C_{plasma-water})/C_{plasma}$, where C_{plasma} was the concentration observed in the noncentrifuged plasma 37 °C sample and $C_{plasma-water}$ was the plasma−water phase following centrifugation.

In Vitro Human and Mouse Metabolism. Human and mouse liver microsomes (BD Gentest, Discovery Labware Inc., Woburn, Massachusetts) were suspended in 0.1 M phosphate buffer (pH 7.4) at a final protein concentration of 0.4 mg/mL and incubated with compounds (1 μM) at 37 °C. An NADPH-regenerating system (1 mg/mL NADP, 1 mg/mL glucose-6-phosphate, 1 U/mL glucose-6-phosphate dehydrogenase) and $MgCl_2$ (0.67 mg/mL) was added to initiate the metabolic reactions, which were subsequently quenched with ice-cold acetonitrile at time points ranging from 0 to 60 min. Samples were also incubated in the absence of the NADPH-regenerating system to monitor for noncytochrome P450-mediated metabolism in the microsomal matrix. Samples were then subjected to centrifugation, and the amount of parent compound remaining in the supernatant was monitored by LC-MS. The first-order rate constant for substrate depletion was determined by fitting the data to an exponential decay function, and these values were used to calculate the in vitro intrinsic clearance value (Cl_{int}) and the predicted in vivo intrinsic clearance value ($CL_{int\ vivo}$) as described.[39] The predicted in vivo hepatic extraction ratio (E_h) was calculated using the following relationship: $E_h = CL_{int\ vivo}/(Q + CL_{int\ vivo})$, where Q is liver blood flow (20.7 mL/min/kg, 55.2 mL/min/kg and 90 mL/min/kg in for humans, rats and mice, respectively).[40]

Pharmacokinetic Analysis. Animal studies were performed in accordance with the Australian Code of Practice for the Care and Use of Animals for Scientific Purposes, and the study protocol was approved by the Monash Institute of Pharmaceutical Sciences Animal Ethics Committee.

Systemic exposure was studied following oral administration of compounds to nonfasted male Swiss outbred mice after oral administration and to overnight fasted male Sprague−Dawley rats after iv and oral administration. Mice were given unrestricted access to food and water throughout the pre- and postdose phases of the study. Rats were given unrestricted access to water throughout the pre- and postdose sampling period, and access to food was reinstated 4 h postdose. For oral dosing, compounds were administered to mice and rats in an aqueous suspension vehicle (0.5% w/v sodium caboxymethylcellulose, 0.5% v/v benzyl alcohol, and 0.4% v/v Tween 80; 0.1 mL dose volume per mouse, n = 1 mouse per time point; 1.0 mL per rat, n = 2 rats per compound) by gavage. After the oral dose was administered to rats, the dosing tube was rinsed with 1 mL of Milli-Q water to collect any residual formulation, and the rinse was also administered. For intravenous dosing to rats, compounds were administered in an aqueous solution vehicle as a 10 min constant rate infusion into the jugular vein at two dose levels (1.0 mL per rat, n = 2 rats per dose level for each compound).

At specific time points following oral dosing to mice, animals were anaesthetized with gaseous isoflurane and a single blood sample was collected via cardiac puncture. For sample collection from rats, samples of arterial blood were collected via an in-dwelling carotid cannula. Blood samples collected from mice and rats were immediately transferred to heparinized tubes that contained a stabilization cocktail (Complete inhibitor cocktail, potassium fluoride, and EDTA) to minimize the potential for ex vivo degradation of the test compound. Plasma for analysis was then collected by centrifugation.

Compound concentrations were quantitated in plasma samples by LC-MS (on either a Micromass Quattro Premier or Micromass Xevo TQ) using calibration standards that were prepared in blank plasma. Plasma samples and standards were prepared by precipitation with acetonitrile, followed by centrifugation and analysis of the supernatant. The analytical lower limit of quantitation (LLQ) value for each compound in plasma was typically 1 ng/mL or below.

Pharmacokinetic parameters were calculated using noncompartmental methods. The terminal elimination half-life ($t_{1/2}$), the area under the plasma concentration versus time profile from time zero to either the last sample time point ($AUC_{0-24\ h}$) or extrapolated to infinity (AUC_{0-inf}), plasma clearance, and volume of distribution at steady-state were determined using WinNonlin software (version 5.2.1, Pharsight Corporation, Mountain View, CA). The maximum plasma concentration (C_{max}), the time to reach the maximum concentration (T_{max}), and the time plasma concentrations remained above 1 μM ($T_{C>1\ \mu M}$) were taken directly from the concentration versus time profiles. Oral bioavailability (%F) was estimated by comparing the average dose-normalized AUC_{0-inf} after oral administration to the average dose-normalized AUC_{0-inf} after iv administration.

***P. falciparum* in Vivo Efficacy Model and Pharmacokinetic Analysis.** All the experiments were approved by the DDW Ethical Committee on Animal Research, performed at the DDW Laboratory Animal Science facilities accredited by AAALAC, and conducted according to European Union legislation and GlaxoSmithKline policy on the care and use of animals.

Compound efficacy was evaluated against *P. falciparum* $Pf3D7^{0087/N9}$ propagated in NOD-*scid* IL-2Rγ^{null} mice that were engrafted with human erythrocytes as previously described.[41] Mice (n = 3) were infected on day 0 with 2×10^7 parasites and compound was administered QD on days 3−6 post infection by oral gavage in an aqueous suspension vehicle (0.5% w/v sodium caboxymethylcellulose, 0.5% v/v benzyl alcohol, and 0.4% v/v Tween 80) at 20 mL/kg. Control animals received vehicle alone. ED_{50} and ED_{90} were estimated by fitting a four-decade logistic equation for the $\log_{10}$ of parasitemia at day 7 versus $\log_{10}$ of the dose administered using GraphPad Prism 5.0 (GrahPad Software). Parasitemia was assessed by FACS as previously described.[28]

In a parallel study, pharmacokinetic properties were also evaluated in the SCID mouse model both in the presence and absence of infection. Compound was administered in a single oral dose of 10 mg/kg and, whole blood levels were followed for 24 h. Analytical methods for the detection of compounds **37** and **38** were as described above. Groups of 3 animals received a single 10 mg/kg oral dose of compound formulated in water/0.5% carboxymethylcellulose/0.4% Tween 80/0.5% benzyl alcohol. Blood samples were collected over 48 h postdosing by puncture of the lateral tail vein and mixed 1:1 with deionized water 0.1% saponin and stored frozen at −70 °C until analysis. After protein precipitation and liquid/liquid extraction, the samples were assayed by LC/MS using ESI conditions by selected ion monitoring in an API 4000 mass spectrometer (Applied Biosystems Sciex, Foster City, CA) coupled to a HPLC chromatograph (Agilent HP1100 series, Agilent Technologies, Spain). Quantification was conducted by comparison to calibration curves prepared in blood. Blood concentration versus time data were analyzed by noncompartmental analysis (NCA) methods using WinNonlin Professional Version 5.2.

Chemistry: Synthetic Methods and Experimental. *General Methods.* Starting materials were obtained from commercial suppliers and used without further purification unless otherwise stated. Flash chromatography was carried out using prepacked Isolute Flash or Biotage silica-gel columns as the stationary phase and analytical grade solvents as the eluent unless otherwise stated.

NMR spectra were determined on a Varian Unity spectrometer. Chemical shifts are reported as δ values (ppm) downfield from tetramethylsilane, used as an internal standard in the solvent indicated. All coupling constants are reported in hertz (Hz), and multiplicities are labeled br (broad), s (singlet), br s (broad singlet), d (doublet), t (triplet), q (quartet), dd (doublet of doublets), dt (doublet of triplets), td (triplet of doublets), ddd (double−doubledoublet), and m (multiplet).

Total ion current traces were obtained for electrospray positive and negative ionization (ES+/ES−) on a Waters ZMD 2000. Analytical

chromatographic conditions used for the LC/MS analysis: Column, ACE, 4.6 mm × 30 mm. The stationary phase particle size is 3 μm, and the flow rate was 1 mL/min. Solvents were A, aqueous solvent = water + 0.1% formic acid; B, organic solvent = acetonitrile + 0.1% formic acid; Methods, 5 min run time (0−0.2 min 10%B, 0.2−3.5 min 10−90% B, 3.5−4.01 min 90% B; 4.01−5 min 90−10% B). The following additional parameters were used: injection volume (5 μL), column temperature (30 °C), UV wavelength range (220−330 nm)

The purity of all tested compounds was ≥95% using the analytical method described above unless stated otherwise.

A table matching the synthetic intermediates to the final compounds is provided as Table S1, Supporting Information.

Synthesis of Compounds 11−55, 100. These compounds were synthesized following the route described in Scheme 1 through intermediates **7**, **8a**−**b**, **9a**−**p**, and **10a**−**p**.

*2,3-Diamino-6-methyl-4(3H)-pyrimidinone (**7**).* To a solution of NaEtO prepared from sodium (9.19 g, 400 mmol) and ethanol (350 mL), aminoguanidine hydrochloride (44.2 g, 400 mmol) was added and the reaction was heated at 50 °C for 30 min. Then, the reaction was filtered to remove NaCl and ethyl 3-oxobutanoate (25.3 mL, 200 mmol) was added to the filtrate, the reaction mixture was heated at reflux for 5 h, and then stirred at RT overnight. The precipitate obtained was filtered and dried under vacuum to afford intermediate **7**, a pale-pink solid (15.2 g, 54% yield). ^{1}H NMR (400 MHz, DMSO-d_6) δ ppm: 7.02 (br s, 2H), 5.51 (br, 1H), 5.29 (s, 2H), 1.98 (s, 3H). ESIMS m/z 141 $(MH)^+$.

*General Procedure for the Synthesis of Compounds **9a**−**9g** and **9j**−**9k**, **9m**−**9o**.* A solution of **7** (2.5 mmol) and the appropriate alkyl chloride (2.5 mmol) in a mixture of 1,4-dioxane (4 mL) and *N*,*N*-dimethylformamide (DMF) (1 mL) was heated at reflux overnight. In cases where the open, uncyclized intermediate was obtained, the reaction mixture was concentrated under vacuum and the crude was dissolved in acetic acid (5 mL) and heated at reflux overnight. The reaction was then concentrated under vacuum, and the residue was purified by flash chromatography on a silica gel column.

*2-Ethyl-5-methyl[1,2,4]triazolo[1,5-a]pyrimidin-7-ol (**9a**).* Eluting with DCM:MeOH mixtures from 100:0 to 90:10% to yield the title compound as a white solid (75% yield). ^{1}H NMR (400 MHz, $CDCl_3$) δ ppm: 5.89 (s, 1H), 2.87 (q, J = 7.4 Hz, 2H), 2.50 (s, 3H), 1.41 (t, J = 7.5 Hz, 3H). ESIMS m/z 179 $(MH)^+$.

*5-Methyl-2-(1-methylethyl)[1,2,4]triazolo[1,5-a]pyrimidin-7-ol (**9b**).* Eluting with DCM:MeOH mixtures, gradient from 100:0 to 90:10% to yield the title compound as a white solid (45% yield). ^{1}H NMR (300 MHz, DMSO-d_6) δ ppm: 13.21−12.82 (br, 1H), 5.76 (s, 1H), 3.06−2.96 (m, 1H), 2.28 (s, 3H), 1.28 (d, J = 6.9 Hz, 6H). ESIMS m/z 193 $(MH)^+$.

*5-Methyl-2-(2-methylpropyl)[1,2,4]triazolo[1,5-a]pyrimidin-7-ol (**9c**).* Eluting with DCM:MeOH mixtures, gradient from 100:0 to 90:10% to yield the title compound as a white solid (46% yield). ^{1}H NMR (300 MHz, DMSO-d_6) δ ppm: 13.01 (br s, 1H), 5.76 (s, 1H), 2.54 (d, J = 7.1 Hz, 2H), 2.49 (s, 3H), 2.09- 2.04 (m, 1H), 0.92 (d, J = 6.6 Hz, 6H). ESIMS m/z 207 $(MH)^+$.

*2-(1,1-Dimethylethyl)-5-methyl[1,2,4]triazolo[1,5-a]pyrimidin-7-ol (**9d**).* Eluting with DCM:MeOH mixtures, gradient from 100:0 to 85:15% to yield the title compound as a white solid (71% yield). ^{1}H NMR (300 MHz, DMSO-d_6) δ ppm: 13.26−12.85 (br, 1H), 5.76 (s, 1H), 2.28 (s, 3H), 1.33 (s, 9H). ESIMS m/z 207 $(MH)^+$.

*5-Methyl-2-(1-methylpropyl)[1,2,4]triazolo[1,5-a]pyrimidin-7-ol (**9e**).* Eluting with DCM:MeOH mixtures, gradient from 99:1 to 85:15% to yield the title compound as a white solid (55% yield). ^{1}H NMR (300 MHz, DMSO-d_6) δ ppm: 13.33−12.78 (br, 1H), 5.76 (s, 1H), 2.85−2.76 (m, 1H), 2.28 (s, 3H), 1.79−1.68 (m, 1H), 1.65−1.55 (m, 1H), 1.25 (d, J = 6.8 Hz, 3H), 0.83 (t, J = 7.3 Hz, 3H). ESIMS m/z 207 $(MH)^+$.

*2-Cyclopropyl-5-methyl[1,2,4]triazolo[1,5-a]pyrimidin-7-ol (**9f**).* Eluting with DCM:MeOH mixtures, gradient from 100:0 to 85:15% to yield the title compound as a white solid (22% yield). ^{1}H NMR (300 MHz, DMSO-d_6) δ ppm: 13.26−12.77 (br, 1H), 5.75 (s, 1H), 2.27 (s, 3H), 2.07 (m, 1H), 1.02−0.97 (m, 2H), 0.9−0.86 (m, 2H). ESIMS m/z 191 $(MH)^-$.

*2-(Cyclopropylmethyl)-5-methyl[1,2,4]triazolo[1,5-a]pyrimidin-7-ol (**9g**).* Eluting with DCM:MeOH mixtures, gradient from 100:0 to 90:10% to yield the title compound as a pale-yellow solid (24% yield). ^{1}H NMR (300 MHz, DMSO-d_6) δ ppm: 13.29−12.92 (br, 1H), 5.76 (s, 1H), 2.59 (d, J = 7.1 Hz, 2H), 2.29 (s, 3H), 1.14−1.03 (m, 1H), 0.50−0.46 (m, 2H), 0.24−0.21 (m, 2H). ESIMS m/z 205 $(MH)^+$.

*5-Methyl-2-[(methyloxy)methyl][1,2,4]triazolo[1,5-a]pyrimidin-7-ol (**9j**).* Eluting with DCM:MeOH mixtures, gradient from 100:0 to 90:10% to yield the title compound as a white solid (87% yield). ^{1}H NMR (300 MHz, DMSO-d_6) δ ppm: 13.01 (br s, 1H), 5.81 (s, 1H), 4.45 (s, 2H), 3.32 (s, 3H), 2.30 (s, 3H). ESIMS m/z 195 $(MH)^+$.

*5-Methyl-2-[2-(methyloxy)ethyl][1,2,4]triazolo[1,5-a]pyrimidin-7-ol (**9k**).* Eluting with DCM:MeOH mixtures, gradient from 100:0 to 90:10% to yield the title compound as a white solid (58% yield). ^{1}H NMR (300 MHz, DMSO-d_6) δ ppm: 13.04 (br s, 1H), 5.77 (s, 1H), 3.70 (t, J = 6.6 Hz, 2H), 3.23 (s, 3H), 2.90 (t, J = 6.6 Hz, 2H), 2.28 (s, 3H). ESIMS m/z 209 $(MH)^+$.

*2-(2-Chloroethyl)-5-methyl[1,2,4]triazolo[1,5-a]pyrimidin-7-ol (**9m**).* Eluting with DCM:MeOH mixtures, gradient from 100:0 to 90:10% to yield the title compound as a white solid (31% yield). ^{1}H NMR (300 MHz, DMSO-d_6) δ ppm: 13.12 (br s, 1H), 5.79 (s, 1H), 3.98 (t, J = 6.6 Hz, 2H), 3.16 (t, J = 6.6 Hz, 2H), 2.29 (s, 3H). ESIMS m/z 213 $(MH)^+$.

*2-(Chloromethyl)-5-methyl-[1,2,4]triazolo[1,5-a]pyrimidin-7-ol (**9n**).* Eluting with DCM:MeOH mixtures, gradient from 100:0 to 90:10% to yield the title compound as a white solid (58% yield). ^{1}H NMR (300 MHz, DMSO-d_6) δ ppm: 13.52−12.72 (br, 1H), 5.85 (s, 1H), 4.78 (s, 2H), 2.32 (s, 3H). ESIMS m/z 199 $(MH)^+$.

*5-Methyl-2-{[(phenylmethyl)oxy]methyl}[1,2,4]triazolo[1,5-a]pyrimidin-7-ol (**9o**).* Eluting with DCM:MeOH mixtures, gradient from 100:0 to 90:10% to yield the title compound as a white solid (72% yield). ^{1}H NMR (400 MHz, DMSO-d_6) δ ppm: 7.27 (m, 5H), 5.84 (s, 1H), 4.76 (s, 2H), 4.55 (s, 2H), 2.45 (s, 3H). ESIMS m/z 271 $(MH)^+$.

*General Procedure for the Synthesis of Compounds **9h** and **9i**.* To a solution of NaEtO prepared from sodium (143 mmol) and ethanol (150 mL), Intermediate **7** (71.4 mmol) was added, and the reaction mixture was heated at 80 °C for 30 min. Then, the reaction mixture was cooled down to RT, and ethyl 2,2-difluoropropanoate (1.2 equiv) or ethyl 2,2-difluorobutanoate (1.2 equiv) were added to synthesize **9h** or **9i**, respectively. The mixture was stirred at RT for 30 min before being heated to 80 °C for 1.5−3 h. The reaction mixture was concentrated to dryness, and water (200 mL) was added. The reaction mixture pH was adjusted to 4 by addition of 2N aq HCl solution while a white solid precipitated. The solid was filtered off, washed with water, and dried under vacuum to afford compounds **9h** or **9i**. The mother liquors were further extracted with DCM (5 × 35 mL), and the combined organic layers were dried over Na_2SO_4, filtered, and concentrated under vacuum to yield additional desired product.

*2-(1,1-Difluoroethyl)-5-methyl[1,2,4]triazolo[1,5-a]pyrimidin-7-ol (**9h**).* White solid (73% yield). ^{1}H NMR (400 MHz, DMSO-d_6) δ ppm: 13.39 (br s, 1H), 5.91 (s, 1H), 2.33 (s, 3H), 2.06 (t, J = 19 Hz, 3H). ESIMS m/z 215 $(MH)^+$.

*2-(1,1-Difluoropropyl)-5-methyl[1,2,4]triazolo[1,5-a]pyrimidin-7-ol (**9i**).* White solid (53% yield). ^{1}H NMR (400 MHz, DMSO-d_6) δ ppm: 13.36 (br s, 1H), 5.90 (s, 1H), 2.40−2.32 (m, 2H), 2.32 (s, 3H), 0.99 (t, J = 7.6 Hz, 3H). ESIMS m/z 229 $(MH)^+$.

*General Procedures for Compounds **9l**, **9p** (Scheme 1). 2-(Trifluoromethyl)-5-methyl-[1,2,4]triazolo[1,5-a]pyrimidin-7-ol (**9l**).* A mixture of ethyl 3-oxobutanoate (20 mmol) and 5-(trifluoromethyl)-4*H*-1,2,4-triazol-3-ylamine **8a** (20 mmol) (commercially

available) was heated under reflux in acetic acid (10 mL) for 4−6 h and then concentrated. The product was then cooled to RT, filtered, washed with water, and dried under vacuum to give a pale-pink solid with 50−65% yield; mp 172−174 °C. ^{1}H NMR (300 MHz, $CDCl_3$): δ ppm: 6.5 (br s, 1H), 6.0 (s, 1H), 2.40 (s, 3H). MS m/z 219.2 $[M + H]^+$.

*3-{2-[(Phenylmethyl)oxy]ethyl}-1H-1,2,4-triazol-5-amine (**8b**).* To a solution of NaEtO prepared from sodium (0.237 g, 10.30 mmol) and ethanol (10 mL), aminoguanidine hydrochloride (1.138 g, 10.30 mmol) was added and the reaction was heated at 50 °C for 30 min. The reaction mixture was filtered to remove NaCl and methyl-3-benzyloxypropanoate (1 g, 5.15 mmol) was added. The reaction mixture was then heated at reflux for 5 h, the formation of product being observed by TLC (90:10 DCM/MeOH) staining with $KMnO_4$. The reaction mixture was concentrated under vacuum, and product was purified by flash chromatography (silica gel column, eluting with DCM/MeOH mixtures from 100:0 to 80:20%). Upon collection of the appropriate fractions, the title compound was obtained as a white solid (0.320 g, 29% yield). ^{1}H NMR (300 MHz, $CDCl_3$) δ ppm: 7.36−7.28 (m, 5H), 4.57 (s, 2H), 3.79 (t, J = 6.6 Hz, 2H), 2.95 (t, J = 6.6 Hz, 2H). ESIMS m/z 219 $(MH)^+$.

*5-Methyl-2-{2-[(phenylmethyl)oxy]ethyl}[1,2,4]triazolo[1,5-a]pyrimidin-7-ol (**9p**).* A solution of Intermediate **8b** (0.31 g, 1.42 mmol) and ethyl 3-oxobutanoate (0.216 mL, 1.704 mmol) in acetic acid (5 mL) was heated at 80 °C overnight. The reaction mixture was concentrated under vacuum to obtain a pale-yellow solid that was triturated in hexane to remove the excess of ethyl 3-oxobutanoate. After drying the solid under vacuum, the title compound was obtained as a pale-yellow solid (0.39 g, 97% yield). ^{1}H NMR (300 MHz, DMSO-d_6) δ ppm: 13.05 (br s, 1H), 7.33−7.24 (m, 5H), 5.77 (s, 1H), 4.49 (s, 2H), 3.81 (t, J = 6.6 Hz, 2H), 2.96 (t, J = 6.6 Hz, 2H), 2.28 (s, 3H). ESIMS m/z 285 $(MH)^+$.

*General Procedure for the Synthesis of Compounds **10a**−**10p**.* A suspension of Intermediate **9a**−**9p** (1.17 mmol) in phosphorus oxychloride (3.5 mmol) was heated at reflux for 1 h. The reaction mixture was added dropwise into iced water, neutralized with solid Na_2CO_3, and product was extracted with DCM. The combined organic layers were washed with brine and dried over anhyd Na_2SO_4. A brown oil was obtained upon solvent removal in vacuo, which was purified by flash chromatography on silica gel, eluting with hexanes:EtOAc mixtures from 100:0 to 40:60%.

*7-Chloro-2-ethyl-5-methyl[1,2,4]triazolo[1,5-a]pyrimidine (**10a**).* White solid (76% yield). ^{1}H NMR (400 MHz, $CDCl_3$) δ ppm: 7.01 (s, 1H), 2.98 (q, J = 7.6 Hz, 2H), 2.68 (s, 3H), 1.43 (t, J = 7.6 Hz, 3H). ESIMS m/z 197 $(MH)^+$.

*7-Chloro-5-methyl-2-(1-methylethyl)[1,2,4]triazolo[1,5-a] pyrimidine (**10b**).* White solid (65% yield). ^{1}H NMR (300 MHz, $CDCl_3$) δ ppm: 7.01 (s, 1H), 3.35−3.25 (m, 1H), 2.68 (s, 3H), 1.45 (d, J = 7.1 Hz, 6H). ESIMS m/z 211 $(MH)^+$.

*7-Chloro-5-methyl-2-(2-methylpropyl)[1,2,4]triazolo[1,5-a]pyrimidine (**10c**).* White solid (85% yield). ^{1}H NMR (300 MHz, $CDCl_3$) δ ppm: 7.01 (s, 1H), 2.82 (d, J = 7.1 Hz, 2H), 2.68 (s, 3H), 2.34−2.29 (m, 1H), 1.45 (d, J = 6.6 Hz, 6H). ESIMS m/z 225 $(MH)^+$.

*7-Chloro-2-(1,1-dimethylethyl)-5-methyl[1,2,4]triazolo[1,5-a]pyrimidine (**10d**).* Pale-yellow solid (58% yield). ^{1}H NMR (300 MHz, $CDCl_3$) δ ppm: 6.99 (s, 1H), 2.67 (s, 3H), 1.50 (s, 9H). ESIMS m/z 225 $(MH)^+$.

*7-Chloro-5-methyl-2-(1-methylpropyl)[1,2,4]triazolo[1,5-a]pyrimidine (**10e**).* Colorless needles (56% yield). ^{1}H NMR (300 MHz, $CDCl_3$) δ ppm: 7.01 (s, 1H), 3.12−3.03 (m, 1H), 2.68 (s, 3H), 2.02−1.91 (m, 1H), 1.81−1.7 (m, 1H), 1.42 (d, J = 7.1 Hz, 3H), 0.93 (t, J = 7.3 Hz, 3H). ESIMS m/z 225 $(MH)^+$.

*7-Chloro-2-cyclopropyl-5-methyl[1,2,4]triazolo[1,5-a]pyrimidine (**10f**).* White solid (13% yield). ^{1}H NMR (300 MHz, $CDCl_3$) δ ppm: 6.97 (s, 1H), 2.66 (s, 3H), 2.28−2.22 (m, 1H), 1.26−1.22 (m, 2H), 1.15−1.10 (m, 2H). ESIMS m/z 209 $(MH)^+$.

*7-Chloro-2-(cyclopropylmethyl)-5-methyl[1,2,4]triazolo[1,5-a]pyrimidine (**10g**).* Yellow solid (36% yield). ^{1}H NMR (300 MHz, DMSO-d_6) δ ppm: 7.57 (s, 1H), 2.76 (d, J = 7.1 Hz, 2H), 2.660 (s, 3H), 1.24−1.12 (m, 1H), 0.52−0.48 (m, 2H), 0.28−0.24 (m, 2H). ESIMS m/z 223 $(MH)^+$.

*7-Chloro-2-(1,1-difluoroethyl)-5-methyl[1,2,4]triazolo[1,5-a] pyrimidine (**10h**).* White solid (86% yield). ^{1}H NMR (400 MHz, $CDCl_3$) δ ppm: 7.17 (s, 1H), 2.75 (s, 3H), 2.18 (t, J = 18.7 Hz, 3H). ESIMS m/z 233 $(MH)^+$.

*7-Chloro-2-(1,1-difluoropropyl)-5-methyl[1,2,4]triazolo[1,5-a] pyrimidine (**10i**).* White solid (68% yield). ^{1}H NMR (400 MHz, $CDCl_3$) δ ppm: 7.17 (s, 1H), 2.75 (s, 3H), 2.53−2.41 (m, 2H), 1.13 (t, J = 7.6 Hz, 3H). ESIMS m/z 247 $(MH)^+$.

*7-Chloro-5-methyl-2-[(methyloxy)methyl][1,2,4]triazolo[1,5-a]pyrimidine (**10j**).* White solid (75% yield). ^{1}H NMR (300 MHz, $CDCl_3$) δ ppm: 7.07 (s, 1H), 4.78 (s, 2H), 3.56 (s, 3H), 2.71 (s, 3H). ESIMS m/z 213 $(MH)^+$.

*7-Chloro-5-methyl-2-[2-(methyloxy)ethyl][1,2,4]triazolo[1,5-a]pyrimidine (**10k**).* White solid (85% yield). ^{1}H NMR (300 MHz, $CDCl_3$) δ ppm: 7.03 (s, 1H), 3.93 (t, J = 6.6 Hz, 2H), 3.38 (s, 3H), 3.24 (t, J = 6.6 Hz, 2H), 2.69 (s, 3H). ESIMS m/z 227 $(MH)^+$.

*7-Chloro-5-methyl-2-(trifluoromethyl)-[1,2,4]triazolo[1,5-a]pyrimidine (**10l**).* Melting point: 102−105 °C. ^{1}H NMR (300 MHz, $CDCl_3$): δ ppm: 7.29 (s, 1H), 2.80 (s, 3H). MS m/z 237.0 $[M + H]^+$.

*7-Chloro-2-(2-chloroethyl)-5-methyl[1,2,4]triazolo[1,5-a]pyrimidine (**10m**).* White solid (67% yield). ^{1}H NMR (300 MHz, $CDCl_3$) δ ppm: 7.06 (s, 1H), 4.04 (t, J = 6.6 Hz, 2H), 3.43 (t, J = 6.6 Hz, 2H), 2.70 (s, 3H). ESIMS m/z 231 $(MH)^+$.

*7-Chloro-2-(chloromethyl)-5-methyl[1,2,4]triazolo[1,5-a]pyrimidine (**10n**).* White solid (65% yield). ^{1}H NMR (300 MHz, $CDCl_3$) δ ppm: 7.11 (s, 1H), 4.82 (s, 2H), 2.73 (s, 3H). ESIMS m/z 217 $(MH)^+$.

*7-Chloro-5-methyl-2-{[(phenylmethyl)oxy]methyl}[1,2,4]triazolo-[1,5-a]pyrimidine (**10o**).* White solid (87% yield). ^{1}H NMR (400 MHz, $CDCl_3$) δ ppm: 7.44−7.35 (m, 5H), 7.07 (s, 1H), 4.84 (s, 2H), 4.77 (s, 2H), 2.71 (s, 3H). ESIMS m/z 289 $(MH)^+$.

*7-Chloro-5-methyl-2-{2-[(phenylmethyl)oxy]ethyl}[1,2,4]triazolo-[1,5-a]pyrimidine (**10p**).* White solid (0.31 g, 75% yield). ^{1}H NMR (300 MHz, $CDCl_3$) δ ppm: 7.33−7.31 (m, 5H), 7.02 (s, 1H), 4.58 (s, 2H), 4.01 (t, J = 6.6 Hz, 2H), 3.28 (t, J = 6.6 Hz, 2H), 2.69 (s, 3H). ESIMS m/z 303 $(MH)^+$.

*General Procedure for the Synthesis of Compounds **11**−**55**, **100**.* To a suspension of Intermediate **10a**−**10p** (1 mmol) in ethanol (5 mL), the corresponding aniline (1 mmol) was added and the mixture was stirred at RT or at 50 °C until the reaction reached completion. Ammonia in methanol (1 mmol) was added and solvent was removed in vacuo and the crude mixture was purified by flash chromatography (silica gel, eluting with hexane:EtOAc mixtures from 75:25 to 25:75%) to yield the title compound.

*N-(4-Chlorophenyl)-2-ethyl-5-methyl[1,2,4]triazolo[1,5-a]pyrimidin-7-amine (**11**).* Pale-yellow solid (87% yield). ^{1}H NMR (400 MHz, DMSO-d_6) δ ppm: 7.55 (d, J = 8.3 Hz, 2H), 7.45 (d, J = 8.3 Hz, 2H), 6.48 (s, 1H), 2.86 (q, J = 7.6 Hz, 2H), 2.43 (s, 3H), 1.34 (t, J = 7.6 Hz, 3H). ESIMS m/z 288 $(MH)^+$.

*N-(3-Chlorophenyl)-2-ethyl-5-methyl[1,2,4]triazolo[1,5-a]pyrimidin-7-amine (**12**).* Pale-yellow solid (82% yield). ^{1}H NMR (400 MHz, DMSO-d_6) δ ppm: 7.54−7.51 (m, 1H), 7.48−7.36 (m, 2H), 6.51 (s, 1H), 2.85 (q, J = 7.6 Hz, 2H), 2.44 (s, 3H), 1.34 (t, J = 7.6 Hz, 3H). ESIMS m/z 288 $(MH)^+$.

*2-Ethyl-5-methyl-N-[4-(trifluoromethyl)phenyl][1,2,4]triazolo[1,5-a]pyrimidin-7-amine (**13**).*[42] White solid (90% yield). ^{1}H NMR (400 MHz, DMSO-d_6) δ ppm: 10.37 (s, 1H), 7.80 (d, J = 8.5 Hz, 2H), 7.66 (d, J = 8.5 Hz, 2H), 6.60 (s, 1H), 2.84 (q, J = 7.6 Hz, 2H), 2.42 (s, 3H), 1.33 (t, J = 7.6 Hz, 3H). ESIMS m/z 322 $(MH)^+$.

*2-Ethyl-5-methyl-N-[4-(pentafluoro-λ^6-sulfanyl)phenyl][1,2,4]triazolo[1,5-a]pyrimidin-7-amine (**14**).*[42] White solid (87% yield). ^{1}H NMR (400 MHz, DMSO-d_6) δ ppm: 10.44 (br s, 1H), 7.95 (d, J = 8.3

Hz, 2H), 7.66 (d, J = 8.3 Hz, 2H), 6.68 (s, 1H), 2.83 (q, J = 7.3 Hz, 2H), 2.43 (s, 3H), 1.32 (t, J = 7.3 Hz, 3H). ESIMS m/z 380 $(MH)^+$.

*N-(4-Chlorophenyl)-5-methyl-2-(1-methylethyl)[1,2,4]triazolo-[1,5-a]pyrimidin-7-amine (**15**).* Colorless solid (35% yield). ^{1}H NMR (300 MHz, $CDCl_3$) δ ppm: 7.77−7.63 (br, 1H), 7.49−7.45 (m, 2H), 7.36−7.31 (m, 2H), 6.27 (s, 1H), 3.29−3.19 (m, 1H), 2.58 (s, 3H), 1.46 (d, J = 7.1 Hz, 6H). ESIMS m/z 302 $(MH)^+$.

*N-(3-Chlorophenyl)-5-methyl-2-(1-methylethyl)[1,2,4]triazolo-[1,5-a]pyrimidin-7-amine (**16**).* White solid (14% yield). ^{1}H NMR (300 MHz, $CDCl_3$) δ ppm: 7.79−7.68 (br, 1H), 7.45−7.39 (m, 2H), 7.33−7.27 (m, 2H), 6.36 (s, 1H), 3.30−3.19 (m, 1H), 2.56 (s, 3H), 1.45 (d, J = 6.9 Hz, 6H). ESIMS m/z 302 $(MH)^+$.

*5-Methyl-2-(1-methylethyl)-N-[4-(trifluoromethyl)phenyl][1,2,4]-triazolo[1,5-a]pyrimidin-7-amine (**17**).*[42] White solid (29% yield). ^{1}H NMR (300 MHz, $CDCl_3$) δ ppm: 8.00−7.86 (br, 1H), 7.77 (d, J = 8.3 Hz, 2H), 7.50 (d, J = 8.3 Hz, 2H), 6.47 (s, 1H), 3.32−3.22 (m, 1H), 2.58 (s, 3H), 1.46 (d, J = 6.9 Hz, 6H). ESIMS m/z 336 $(MH)^+$.

*5-Methyl-2-(1-methylethyl)-N-[4-(pentafluoro-λ^6-sulfanyl)phenyl]-[1,2,4]triazolo[1,5-a]pyrimidin-7-amine (**18**).*[42] White solid (35% yield). ^{1}H NMR (300 MHz, $CDCl_3$) δ ppm: 7.96−7.83 (br, 3H), 7.47 (d, J = 8.8 Hz, 2H), 6.50 (s, 1H), 3.30−3.20 (m, 1H), 2.58 (s, 3H), 1.45 (d, J = 6.9 Hz, 6H). ESIMS m/z 394 $(MH)^+$.

*N-(4-Chlorophenyl)-5-methyl-2-(2-methylpropyl)[1,2,4]triazolo-[1,5-a]pyrimidin-7-amine (**19**).* White solid (87% yield). ^{1}H NMR (400 MHz, DMSO-d_6) δ ppm: 10.15 (s, 1H), 7.50 (d, J = 8.3 Hz, 2H), 7.46 (d, J = 8.3 Hz, 2H), 6.36 (s, 1H), 2.66 (d, J = 7.1 Hz, 2H), 2.38 (s, 3H), 2.26−2.22 (m, 1H), 0.96 (d, J = 6.6 Hz, 6H). ESIMS m/z 316 $(MH)^+$.

*N-(3-Chlorophenyl)-5-methyl-2-(2-methylpropyl)[1,2,4]triazolo-[1,5-a]pyrimidin-7-amine (**20**).* White solid (88% yield). ^{1}H NMR (400 MHz, DMSO-d_6) δ ppm: 10.39 (s, 1H), 7.79 (d, J = 7.9 Hz, 2H), 7.67 (d, J = 7.3 Hz, 2H), 6.60 (s, 1H), 2.67 (d, J = 7.1 Hz, 2H), 2.42 (s, 3H), 2.21−2.17 (m, 1H), 0.96 (d, J = 6.6 Hz, 6H). ESIMS m/z 316 $(MH)^+$.

*5-Methyl-2-(2-methylpropyl)-N-[4-(trifluoromethyl)phenyl][1,2,4]-triazolo[1,5-a]pyrimidin-7-amine (**21**).*[42] White solid (96% yield). ^{1}H NMR (400 MHz, DMSO-d_6) δ ppm: 10.19 (s, 1H), 7.55−7.41 (m, 3H), 7.33−7.31 (m, 1H), 6.41 (s, 1H), 2.67 (d, J = 7.1 Hz, 2H), 2.40 (s, 3H), 2.20−2.17 (m, 1H), 0.96 (d, J = 6.6 Hz, 6H). ESIMS m/z 350 $(MH)^+$.

*5-Methyl-2-(2-methylpropyl)-N-[4-(pentafluoro-λ^6-sulfanyl)phenyl]-[1,2,4]triazolo[1,5-a]pyrimidin-7-amine (**22**).*[42] White solid (92% yield). ^{1}H NMR (400 MHz, DMSO-d_6) δ ppm: 10.45 (s, 1H), 7.95 (d, J = 8.7 Hz, 2H), 7.66 (d, J = 8.7 Hz, 2H), 6.67 (s, 1H), 2.68 (d, J = 7.1 Hz, 2H), 2.43 (s, 3H), 2.22−2.17 (m, 1H), 0.96 (d, J = 6.6 Hz, 6H). ESIMS m/z 408 $(MH)^+$.

*2-(1,1-Dimethylethyl)-5-methyl-N-[4-(trifluoromethyl)phenyl]-[1,2,4]triazolo[1,5-a]pyrimidin-7-amine (**23**).* White foam (66% yield). ^{1}H NMR (300 MHz, DMSO-d_6) δ ppm: 10.15−10.04 (br, 1H), 7.81 (d, J = 8.6 Hz, 2H), 7.69−7.67 (m, 2H), 6.54 (s, 1H), 2.41 (s, 3H). 1.43 (s, 9H). ESIMS m/z 350 $(MH)^+$.

*2-(1,1-Dimethylethyl)-5-methyl-N-[4-(pentafluoro-λ^6-sulfanyl)-phenyl][1,2,4]triazolo[1,5-a]pyrimidin-7-amine (**24**).* White solid (49% yield). ^{1}H NMR (300 MHz, DMSO-d_6) δ ppm: 10.2−10.08 (br, 1H), 7.96 (d, J = 9.1 Hz, 2H), 7.75−7.62 (m, 2H), 6.53 (s, 1H), 2.42 (s, 3H), 1.43 (s, 9H). ESIMS m/z 408 $(MH)^+$.

*5-Methyl-2-(1-methylpropyl)-N-[4-(trifluoromethyl)phenyl][1,2,4]-triazolo[1,5-a]pyrimidin-7-amine (**25**).* White solid (35% yield). ^{1}H NMR (300 MHz, DMSO-d_6) δ ppm: 10.41−10.3 (br, 1H), 7.8 (d, J = 8.3 Hz, 2H), 7.69−7.67 (m, 2H), 6.59 (s, 1H), 2.98−2.89 (m, 1H), 2.42 (s, 3H), 1.9−1.79 (m, 1H), 1.73−1.62 (m, 1H), 1.33 (d, J = 7.07 Hz, 3H), 0.86 (t, J = 7.3 Hz, 3H). ESIMS m/z 350 $(MH)^+$.

*5-Methyl-2-(1-methylpropyl)-N-[4-(pentafluoro-λ^6-sulfanyl)phenyl]-[1,2,4]triazolo[1,5-a]pyrimidin-7-amine (**26**).* White solid (39% yield). ^{1}H NMR (300 MHz, DMSO-d_6) δ ppm: 10.49−10.31 (br, 1H), 7.97−7.95 (m, 2H), 7.68−7.66 (m, 2H), 6.67 (s, 1H), 2.98−2.89 (m, 1H), 2.43 (s, 3H), 1.9−1.79 (m, 1H), 1.73−1.62 (m, 1H), 1.32 (d, J = 7.07 Hz, 3H), 0.88−0.84 (m, 3H). ESIMS m/z 408 $(MH)^+$.

*N-(4-Chlorophenyl)-2-cyclopropyl-5-methyl[1,2,4]triazolo[1,5-a]-pyrimidin-7-amine (**27**).* White solid (69% yield). ^{1}H NMR (300 MHz, DMSO-d_6) δ ppm: 10.66−10.25 (br, 1H), 7.55−7.52 (m, 2H), 7.48−7.45 (m, 2H), 6.40 (s, 1H), 2.39 (s, 3H), 2.20−2.13 (m, 1H), 1.11−1.01 (m, 4H). ESIMS m/z 300 $(MH)^+$.

*N-(3-Chlorophenyl)-2-cyclopropyl-5-methyl-[1,2,4]triazolo[1,5-a]-pyrimidin-7-amine (**28**).* Beige solid (82% yield). ^{1}H NMR (300 MHz, DMSO-d_6) δ ppm: 10.53−10.26 (br, 1H), 7.52−7.48 (m, 2H), 7.45−7.42 (m, 1H), 7.38−7.35 (m, 1H), 6.45 (s, 1H), 2.41 (s, 3H), 2.20−2.13 (m, 1H), 1.10−1.01 (m, 4H). ESIMS m/z 300 $(MH)^+$.

*2-Cyclopropyl-5-methyl-N-[4-(trifluoromethyl)phenyl][1,2,4]-triazolo[1,5-a]pyrimidin-7-amine (**29**).*[42] White solid (26% yield). ^{1}H NMR (300 MHz, DMSO-d_6) δ ppm: 10.79−10.36 (br, 1H), 7.82 (d, J = 8.34 Hz, 2H), 7.67 (d, J = 8.34 Hz, 2H), 6.62 (s, 1H), 2.42 (s, 3H), 2.21−2.14 (m, 1H), 1.11−1.01 (m, 4H). ESIMS m/z 334 $(MH)^+$.

*2-Cyclopropyl-5-methyl-N-[4-(pentafluoro-l^6-sulfanyl)phenyl]-[1,2,4]triazolo[1,5-a]pyrimidin-7-amine (**30**).*[42] Beige solid (60% yield). ^{1}H NMR (300 MHz, DMSO-d_6) δ ppm: 10.89−10.35 (br, 1H), 8.01−7.95 (m, 2H), 7.66 (d, J = 8.8 Hz, 2H), 6.69 (s, 1H), 2.43 (s, 3H), 2.20−2.14 (m, 1H), 1.10−1.01 (m, 4H). ESIMS m/z 392 $(MH)^+$.

*N-(4-Chlorophenyl)-2-(cyclopropylmethyl)-5-methyl-[1,2,4]triazolo-[1,5-a]pyrimidin-7-amine (**31**).* White solid (60% yield). ^{1}H NMR (300 MHz, DMSO-d_6) δ ppm: 10.65−10.29 (br, 1H), 7.56−7.53 (m, 2H), 7.49−7.45 (m, 2H), 6.44 (s, 1H), 2.76 (d, J = 6.8 Hz, 2H), 2.42 (s, 3H), 1.24−1.14 (m, 1H), 0.54−0.50 (m, 2H), 0.31−0.27 (m, 2H). ESIMS m/z 314 $(MH)^+$.

*N-(3-Chlorophenyl)-2-(cyclopropylmethyl)-5-methyl-[1,2,4]triazolo-[1,5-a]pyrimidin-7-amine (**32**).* White solid (75% yield). ^{1}H NMR (300 MHz, DMSO-d_6) δ ppm: 10.65−10.28 (br, 1H), 7.53−7.49 (m, 2H), 7.46−7.43 (m, 1H), 7.38−7.36 (m, 1H), 6.48 (s, 1H), 2.75 (d, J = 71 Hz, 2H), 2.43 (s, 3H), 1.24−1.15 (m, 1H), 0.54−0.49 (m, 2H), 0.31−0.27 (m, 2H). ESIMS m/z 314 $(MH)^+$.

*2-(Cyclopropylmethyl)-5-methyl-N-(4-(trifluoromethyl)phenyl)-[1,2,4]triazolo[1,5-a]pyrimidin-7-amine (**33**).* White solid (11% yield). ^{1}H NMR (300 MHz, DMSO-d_6) δ ppm: 10.77−10.36 (br, 1H), 7.82 (d, J = 8.5 Hz, 2H), 7.68 (d, J = 8.5 Hz, 2H), 6.64 (s, 1H), 2.76 (d, J = 7.1 Hz, 2H), 2.44 (s, 3H), 1.25−1.14 (m, 1H), 0.54−0.49 (m, 2H), 0.30−0.27 (m, 2H). ESIMS m/z 348 $(MH)^+$.

*2-(Cyclopropylmethyl)-5-methyl-N-(4-(pentafluoro-λ^6-sulfanyl)-phenyl]-[1,2,4]triazolo[1,5-a]pyrimidin-7-amine (**34**).* White solid (14% yield). ^{1}H NMR (300 MHz, DMSO-d_6) δ ppm: 10.67−10.38 (br, 1H), 7.99−7.95 (m, 2H), 7.67 (d, J = 8.8 Hz, 2H), 6.70 (s, 1H), 2.75 (d, J = 7.1 Hz, 2H), 2.45 (s, 3H), 1.25−1.14 (m, 1H), 0.53−0.49 (m, 2H), 0.30−0.26 (m, 2H). ESIMS m/z 406 $(MH)^+$.

*N-(4-Chlorophenyl)-2-(1,1-difluoroethyl)-5-methyl[1,2,4]triazolo-[1,5-a]pyrimidin-7-amine (**35**).* Beige solid (91% yield). ^{1}H NMR (400 MHz, DMSO-d_6) δ ppm: 10.35 (s, 1H), 7.53 (d, J = 8.3 Hz, 2H), 7.46 (d, J = 8.3 Hz, 2H), 6.45 (s, 1H), 2.42 (s,3H), 2.12 (t, J = 18.7 Hz, 3H). ESIMS m/z 324 $(MH)^+$.

*N-(3-Chlorophenyl)-2-(1,1-difluoroethyl)-5-methyl[1,2,4]triazolo-[1,5-a]pyrimidin-7-amine (**36**).*[42] Beige solid (91% yield). ^{1}H NMR (400 MHz, DMSO-d_6) δ ppm: 10.39 (s, 1H), 7.53−7.47 (m, 3H), 7.45−6.36 (m, 1H), 6.52 (s, 1H), 2.44 (s, 3H), 2.13 (t, J = 18.8 Hz, 3H). ESIMS m/z 324 $(MH)^+$.

*2-(1,1-Difluoroethyl)-5-methyl-N-[4-(trifluoromethyl)phenyl]-[1,2,4]triazolo[1,5-a]pyrimidin-7-amine (**37**).*[42] White solid (81% yield). ^{1}H NMR (300 MHz, DMSO-d_6) δ ppm: 10.58 (s, 1H), 7.83 (d, J = 8.5 Hz, 2H), 7.70 (d, J = 8.5 Hz, 2H), 6.73 (s, 1H), 2.47 (s, 3H), 2.14 (t, J = 18.8 Hz, 3H). ESIMS m/z 358 $(MH)^+$.

*2-(1,1-Difluoroethyl)-5-methyl-N-[4-(pentafluoro-λ^6-sulfanyl)phenyl]-[1,2,4]triazolo[1,5-a]pyrimidin-7-amine (**38**).*[42] White solid (81% yield).

^{1}H NMR (400 MHz, DMSO-d_6) δ ppm: 10.60 (br s, 1H), 7.97 (d, J = 9.3 Hz, 2H), 7.67 (d, J = 9.1 Hz, 2H), 6.79 (s, 1H), 2.47 (s, 3H), 2.13 (t, J = 18.9 Hz, 3H). ESIMS m/z 416 $(MH)^+$.

N-(4-Chlorophenyl)-2-(1,1-difluoropropyl)-5-methyl[1,2,4]triazolo-[1,5-a]pyrimidin-7-amine (**39**). White solid (88% yield). ^{1}H NMR (400 MHz, DMSO-d_6) δ ppm: 10.34 (s, 1H), 7.53 (d, J = 8.3 Hz, 2H), 7.48 (d, J = 8.3 Hz, 2H), 6.47 (s, 1H), 2.42−2.39 (m, 5H), 1.02 (t, J = 7.3 Hz, 3H). ESIMS m/z 338 $(MH)^+$.

N-(3-Chlorophenyl)-2-(1,1-difluoropropyl)-5-methyl[1,2,4]triazolo-[1,5-a]pyrimidin-7-amine (**40**). White solid (77% yield). ^{1}H NMR (400 MHz, DMSO-d_6) δ ppm: 10.38 (s, 1H), 7.54−7.48 (m, 3H), 7.38−7.36 (m, 1H), 6.52 (s, 1H), 2.44−2.39 (m, 5H), 1.02 (t, J = 7.3 Hz, 3H). ESIMS m/z 338 $(MH)^+$.

2-(1,1-Difluoropropyl)-5-methyl-N-[4-(trifluoromethyl)phenyl]-[1,2,4]triazolo[1,5-a]pyrimidin-7-amine (**41**).[42] White solid (83% yield). ^{1}H NMR (400 MHz, DMSO-d_6) δ ppm: 10.58 (br s, 1H), 7.82 (d, J = 8.5 Hz, 2H), 7.67 (d, J = 8.4 Hz, 2H), 6.69 (s, 1H), 2.45 (s, 3H), 2.43−2.37 (m, 2H), 1.02 (t, J = 7.6 Hz, 3H). ESIMS m/z 372 $(MH)^+$.

2-(1,1-Difluoropropyl)-5-methyl-N-[4-(pentafluoro-λ^6-sulfanyl)-phenyl][1,2,4]triazolo[1,5-a]pyrimidin-7-amine (**42**).[42] ^{1}H NMR (400 MHz, DMSO-d_6) δ ppm: 10.63 (br s, 1H), 7.97 (d, J = 9.0 Hz, 2H), 7.67 (d, J = 8.7 Hz, 2H), 6.78 (s, 1H), 2.47 (s, 3H), 2.45−2.37 (m, 2H), 1.02 (t, J = 7.3 Hz, 3H).ESIMS m/z 430 $(MH)^+$; mp 132−134 °C.

2-(Trifluoromethyl)-N-(4-(trifluoromethyl)phenyl)-5-methyl-[1,2,4]triazolo[1,5-a]pyrimidin-7-amine (**43**).[42] Products were purified by column chromatography with 15−20% EtOAc/hexane. Yields ranged from 20−30%; mp 124−126 °C. ^{1}H NMR (300 MHz, $CDCl_3$): δ 7.93 (brs, NH, exchangeable), 7.82 (d, J = 8.1 Hz, 2H), 7.54 (d, J = 8.7 Hz, 2H), 6.61 (s, 1H), 2.65 (s, 3H). MS m/z 362.3 $[MH]^+$.

2-(Trifluoromethyl)-N-(4-(sulfurpentafluoro)phenyl)-5-methyl-[1,2,4]triazolo[1,5-a]pyrimidin-7-amine (**44**).[42] Products were purified by column chromatography with 15−20% EtOAc/hexane. Yields ranged from 20−30%; mp 178−180 °C. ^{1}H NMR (300 MHz, $CDCl_3$): δ 10.79 (brs, NH, exchangeable), 8.01 (d, J = 8.9 Hz, 2H), 7.70 (d, J = 9.2 Hz, 2H), 6.90 (s, 1H), 2.51 (s, 3H). MS m/z 420.3 $[MH]^+$.

2-(Chloromethyl)-N-(4-chlorophenyl)-5-methyl[1,2,4]triazolo-[1,5-a]pyrimidin-7-amine (**45a**). Brown foam (82% yield). ^{1}H NMR (300 MHz, $CDCl_3$) δ ppm: 7.97−7.63 (br, 1H), 7.51−7.46 (m, 2H), 7.35−7.30 (m, 2H), 6.33 (s, 1H), 4.80 (s, 2H), 2.56 (s, 3H). ESIMS m/z 308 $(MH)^+$.

2-(Chloromethyl)-N-(3-chlorophenyl)-5-methyl-[1,2,4]triazolo-[1,5-a]pyrimidin-7-amine (**45b**). Orange oil (91% yield). ^{1}H NMR (300 MHz, $CDCl_3$) δ ppm: 7.96−7.67 (br, 1H), 7.48−7.39 (m, 2H), 7.36−7.27 (m, 2H), 6.41 (s, 1H), 4.80 (s, 2H), 2.59 (s, 3H); m/z 308 $(MH)^+$.

2-(2-Chloroethyl)-N-(4-chlorophenyl)-5-methyl[1,2,4]triazolo-[1,5-a]pyrimidin-7-amine (**46a**). White solid (81% yield). ^{1}H NMR (300 MHz, $CDCl_3$) δ ppm: 7.69 (s, 1H), 7.46 (d, J = 8.3 Hz, 2H), 7.29 (d, J = 8.3 Hz, 2H), 6.29 (s, 1H), 4.04 (t, J = 6.6 Hz, 2H), 3.37 (t, J = 6.6 Hz, 2H), 2.53 (s, 3H). ESIMS m/z 322 $(MH)^+$.

2-(2-Chloroethyl)-N-(3-chlorophenyl)-5-methyl[1,2,4]triazolo[1,5-a]-pyrimidin-7-amine (**46b**). White solid (96% yield). ^{1}H NMR (300 MHz, $CDCl_3$) δ ppm: 7.76 (s, 1H), 7.43−7.28 (m 4 H), 6.38 (s, 1H), 4.04 (t, J = 6.6 Hz, 2H), 3.38 (t, J = 6.6 Hz, 2H), 2.56 (s, 3H). ESIMS m/z 322 $(MH)^+$.

N-(4-Chlorophenyl)-5-methyl-2-{[(phenylmethyl)oxy]methyl}[1,2,4]-triazolo[1,5-a]pyrimidin-7-amine (**47a**). Pale-yellow solid (96% yield). ^{1}H NMR (400 MHz, DMSO-d_6) δ ppm: 7.56 (d, J = 8.3 Hz, 2H), 7.47 (d, J = 8.3 Hz, 2H), 7.36−7.20 (m, 5H), 6.50 (s, 1H), 4.75 (s, 2H), 4.65 (s, 2H), 2.45 (s, 3H). ESIMS m/z 380 $(MH)^+$.

N-(3-Chlorophenyl)-5-methyl-2-{[(phenylmethyl)oxy]methyl}-[1,2,4]triazolo[1,5-a]pyrimidin-7-amine (**47b**). Pale-yellow solid (97% yield). ^{1}H NMR (400 MHz, DMSO-d_6) δ ppm: 7.52−7.30 (m, 9H), 6.54 (s, 1H), 4.75 (s, 2H), 4.65 (s, 2H), 2.46 (s, 3H). ESIMS m/z 380 $(MH)^+$.

N-(4-Chlorophenyl)-5-methyl-2-[(methyloxy)methyl][1,2,4]triazolo-[1,5-a]pyrimidin-7-amine (**48**). White solid (70% yield). ^{1}H NMR (400 MHz, DMSO-d_6) δ ppm: 10.28 (s, 1H), 7.52 (d, J = 8.3 Hz, 2H), 7.46 (d, J = 8.3 Hz, 2H), 6.41 (s, 1H), 4.59 (s, 2H), 3.37 (s, 3H), 2.40 (s, 3H). ESIMS m/z 304 $(MH)^+$.

N-(3-Chlorophenyl)-5-methyl-2-[(methyloxy)methyl][1,2,4]triazolo-[1,5-a]pyrimidin-7-amine (**49**). White solid (79% yield). ^{1}H NMR (400 MHz, DMSO-d_6) δ ppm: 10.32 (s, 1H), 7.51−7.45 (m, 3H), 7.35−7.32 (m, 1H), 6.46 (s, 1H), 4.60 (s, 2H), 3.37 (s, 3H), 2.42 (s, 3H). ESIMS m/z 304 $(MH)^+$.

5-Methyl-2-[(methyloxy)methyl]-N-[4-(trifluoromethyl)phenyl]-[1,2,4]triazolo[1,5-a]pyrimidin-7-amine (**50**). Pale-yellow solid (90% yield). ^{1}H NMR (400 MHz, DMSO-d_6) δ ppm: 10.52 (s, 1H), 7.81 (d, J = 8.5 Hz, 2H), 7.68 (d, J = 8.5 Hz, 2H, 6.66 (s, 1H), 4.61 (s, 1H), 3.38 (s, 3H), 2.44 (s, 3H). ESIMS m/z 338 $(MH)^+$.

5-Methyl-2-[(methyloxy)methyl]-N-[4-(pentafluoro-λ^6-sulfanyl)-phenyl][1,2,4]triazolo[1,5-a]pyrimidin-7-amine (**51**). White solid (92% yield). ^{1}H NMR (400 MHz, DMSO-d_6) δ ppm: 10.59 (s, 1H), 7.98 (d, J = 8.7 Hz, 2H), 7.69 (d, J = 8.7 Hz, 2H), 6.75 (s, 1H), 4.63 (s, 2H), 3.39 (s, 3H), 2.47 (s, 3H). ESIMS m/z 396 $(MH)^+$.

N-(4-Chlorophenyl)-5-methyl-2-[2-(methyloxy)ethyl][1,2,4]triazolo-[1,5-a]pyrimidine-7-amine (**52**). White solid (93% yield). ^{1}H NMR (400 MHz, DMSO-d_6) δ ppm: 10.17 (s, 1H), 7.51 (d, J = 7.3 Hz, 2H), 7.45 (d, J = 7.3 Hz, 2H), 6.37 (s, 1H), 3.78 (t, J = 6.6 Hz, 2H), 3.25 (s, 3H), 3.03 (t, J = 6.6 Hz, 2H), 2.38 (s, 3H). ESIMS m/z 318 $(MH)^+$.

N-(3-Chlorophenyl)-5-methyl-2-[2-(methyloxy)ethyl][1,2,4]triazolo-[1,5-a]pyrimidin-7-amine (**53**). White solid (55% yield). ^{1}H NMR (400 MHz, DMSO-d_6) δ ppm: 10.19 (s, 1H), 7.51−7.46 (m, 2H), 7.37−7.34 (m, 1H), 6.42 (s, 1H), 3.79 (t, J = 6.6 Hz, 2H), 3.25 (s, 3H), 3.03 (t, J = 6.6 Hz, 2H), 2.40 (s, 3H). ESIMS m/z 318 $(MH)^+$.

5-Methyl-2-[2-(methyloxy)ethyl]-N-[4-(trifluoromethyl)phenyl]-[1,2,4]triazolo[1,5-a]pyrimidin-7-amine (**54**). White solid (86% yield). ^{1}H NMR (400 MHz, DMSO-d_6) δ ppm: 10.42 (s, 1H), 7.80 (d, J = 8.5 Hz, 2H), 7.66 (d, J = 8.5 Hz, 2H), 6.61 (s, 1H), 3.79 (t, J = 6.6 Hz, 2H), 3.25 (s, 3H), 3.04 (t, J = 6.6 Hz, 2H), 2.42 (s, 3H). ESIMS m/z 352 $(MH)^+$.

5-Methyl-2-[2-(methyloxy)ethyl]-N-[4-(pentafluoro-λ^6-sulfanyl)-phenyl][1,2,4]triazolo[1,5-a]pyrimidin-7-amine (**55**). White solid (72% yield). ^{1}H NMR (400 MHz, DMSO-d_6) δ ppm: 10.48 (s, 1H), 7.96 (d, J = 8.7 Hz, 2H), 7.66 (d, J = 8.7 Hz, 2H), 6.69 (s, 1H), 3.79 (t, J = 6.6 Hz, 2H), 3.25 (s, 3H), 3.04 (t, J = 6.6 Hz, 2H), 2.43 (s, 3H). ESIMS m/z 410 $(MH)^+$.

Synthesis of Compounds 66−84. These compounds were synthesized following the route described in Scheme 2 through intermediates **56**−**65**.

7-Chloro-5-methyl-2-(methylthio)[1,2,4]triazolo[1,5-a]pyrimidine (**57**). A suspension of commercially available 7-hydroxy-5-methyl-2-methylthio-*S*-triazolo[1,5-*a*]pyrimidine (**56**) (2 g, 10.19 mmol) in phosphorus oxychloride (5 mL, 53.6 mmol) was heated at reflux for 10 h, the starting material solubilizing and the mixture turning bright orange. TLC analysis (hexane/EtOAC 1:1) showed a very messy reaction that had not reached completion, but it was decided to stop it to prevent further product degradation. Hence, the reaction mixture was added dropwise to iced water. The solution was neutralized with aq 1N Na_2CO_3, and product was extracted with DCM. The aqueous layer was further extracted with DCM, and the combined organic layers were washed with brine and dried over anhyd Na_2SO_4. Solvent was removed under reduced pressure, yielding a reddish solid which was purified by flash chromatography (silica gel, eluting with hexane/EtOAc mixtures from 95:5 to 40:60%). Upon collection of the appropriate fractions, the title compound was obtained as a white solid (1.09 g, 47% yield).

^{1}H NMR (300 MHz, $CDCl_3$) δ ppm: 6.99 (s, 1H), 2.74 (s, 3H), 2.68 (s, 3H). ESIMS m/z 215 $(MH)^+$.

General Procedures for the Synthesis of Compounds ***58*****–*****61***. To a suspension of intermediate **57** (1 mmol) in ethanol (10 mL), the appropriate aniline (1 mmol) was added and the mixture was stirred at RT until reaching completion. Anhydrous ammonia (7 M solution in MeOH, 1 mmol) was then added to the mixture and solvent was removed in vacuo. The crude mixture was purified by flash chromatography (silica gel, eluting with hexane/EtOAc mixtures from 95:5 to 40:60%).

*N-(4-Chlorophenyl)-5-methyl-2-(methylthio)[1,2,4]triazolo[1,5-a]pyrimidin-7-amine (****58****).* Beige solid (86% yield). ^{1}H NMR (300 MHz, DMSO-d_6) δ ppm: 10.81–10.15 (br, 1H), 7.57–7.54 (m, 2H), 7.48–7.45 (m, 2H), 6.42 (s, 1H), 2.69 (s, 3H), 2.42 (s, 3H). ESIMS m/z 306 $(MH)^+$.

*N-(3-Chlorophenyl)-5-methyl-2-(methylthio)[1,2,4]triazolo[1,5-a]pyrimidin-7-amine (****59****).* Pale-yellow solid (61% yield). ^{1}H NMR (300 MHz, DMSO-d_6) δ ppm: 11.26–10.10 (br, 1H), 7.55–7.5 (m, 2H), 7.45–7.39 (m, 2H), 6.48 (s, 1H), 2.69 (s, 3H), 2.44 (s, 3H). ESIMS m/z 306 $(MH)^+$.

*5-Methyl-2-(methylthio)-N-[4-(trifluoromethyl)phenyl][1,2,4]triazolo[1,5-a]pyrimidin-7-amine (****60****).*[42] White solid (86% yield). ^{1}H NMR (300 MHz, DMSO-d_6) δ ppm: 10.33 (s, 1H), 7.81 (d, J = 8.3 Hz, 2H), 7.67 (d, J = 8.3 Hz, 2H), 6.62 (s, 1H), 2.68 (s, 3H), 2.42 (s, 3H). ESIMS m/z 340 $(MH)^+$.

*5-Methyl-2-(methylthio)-N-[4-(pentafluoro-λ^6-sulfanyl)phenyl][1,2,4]triazolo[1,5-a]pyrimidin-7-amine (****61****)*[42]. Light-yellow solid (72% yield). ^{1}H NMR (300 MHz, DMSO-d_6) δ ppm: 10.39 (s, 1H), 7.98–7.96 (m, 2H), 7.66 (d, J = 8.8 Hz, 2H), 6.70 (s, 1H), 2.68 (s, 3H), 2.44 (s, 3H). ESIMS m/z 398 $(MH)^+$.

General Procedures for the Synthesis of Compounds ***62*****–*****65*** *(Scheme 2).* To a mixture of the corresponding derivative **58**–**61** (1 mmol) and acetic acid (7 mL), sodium tungstate dihydrate (0.034 mmol) was added at RT. The reaction mixture was vigorously stirred and hydrogen peroxide (2 mmol) was added slowly at 40 °C. The resulting mixture was then heated at 50 °C until reaching completion. The excess hydrogen peroxide was destroyed by the addition of an aqueous solution of sodium sulfite, product being extracted with DCM several times. The combined organic layers were washed with brine and dried over anhydrous Na_2SO_4. A white solid was obtained upon solvent removal in vacuo which was purified by flash chromatography (silica gel, eluting with hexane/EtOAc mixtures from 95:5% to 0:100%).

*N-(4-Chlorophenyl)-5-methyl-2-(methylsulfonyl)[1,2,4]triazolo[1,5-a]pyrimidin-7-amine (****62****).* White solid (36% yield). ^{1}H NMR (300 MHz, DMSO-d_6) δ ppm: 10.58 (s, 1H), 7.57–7.54 (m, 2H), 7.50–7.47 (m, 2H), 6.57 (s, 1H), 3.48 (s, 3H), 2.46 (s, 3H). ESIMS m/z 338 $(MH)^+$.

*N-(3-Chlorophenyl)-5-methyl-2-(methylsulfonyl)[1,2,4]triazolo[1,5-a]pyrimidin-7-amine (****63****).* White solid (35% yield). ^{1}H NMR (300 MHz, DMSO-d_6) δ ppm: 10.62 (br s, 1H), 7.55–7.37 (m, 4H), 6.62 (s, 1H), 3.48 (s, 3H), 2.48 (s, 3H). ESIMS m/z 338 $(MH)^+$.

*5-Methyl-2-(methylsulfonyl)-N-[4-(trifluoromethyl)phenyl][1,2,4]triazolo[1,5-a]pyrimidin-7-amine (****64****).* White solid (56% yield). ^{1}H NMR (300 MHz, $CDCl_3$) δ ppm: 8.18 (br s, 1H), 7.81–7.79 (m, 2H), 7.53 (d, J = 8.3 Hz, 2H), 6.63 (s, 1H), 3.44 (s, 3H), 2.64 (s, 3H). ESIMS m/z 372 $(MH)^+$.

*5-Methyl-2-(methylsulfonyl)-N-[4-(pentafluoro-λ^6-sulfanyl)phenyl][1,2,4]triazolo[1,5-a]pyrimidin-7-amine (****65****).* White solid (51% yield). ^{1}H NMR (300 MHz, $CDCl_3$) δ ppm: 8.23–8.10 (br s, 1H), 7.93–7.91 (m, 2H), 7.50 (d, J = 8.6 Hz, 2H), 6.67 (s, 1H), 3.44 (s, 3H), 2.66 (s, 3H). ESIMS m/z 430 $(MH)^+$.

General Procedures for the Synthesis of Compounds ***66*****–*****86*** *(Scheme 2).* The appropriate derivative **62**–**65** (0.15 g, 0.349 mmol) was added to sodium methoxide (3 mmol) in methanol (9 mL) (**66**, **67**), or sodium ethoxide (3 mmol) in ethanol (9 mL) (**68**–**71**), or to the appropriate alcohol (1.2 mmol) with sodium hydride (2 mmol) in THF (7 mL) (**72**–**84**). The mixture was heated under microwave irradiation at 120 °C for 0.5–1 h. Solvent was removed under vacuum, and the crude mixture was purified by flash chromatography (silica gel, eluting with DCM: MeOH mixtures from 100:0 to 90:10%) or preparative HPLC (SunFire 30 mm × 250 mm, H_2O 0.1% TFA–ACN 0.1% TFA gradient from 20 to 80%).

*N-(3-Chlorophenyl)-5-methyl-2-(methyloxy)[1,2,4]triazolo[1,5-a]pyrimidin-7-amine (****66****).* White solid (33% yield). ^{1}H NMR (300 MHz, DMSO-d_6) δ ppm: 10.44–9.95 (br, 1H), 7.52–7.41 (m, 3H), 7.37–7.34 (m, 1H), 6.43 (s, 1H), 4.06 (s, 3H), 2.39 (s, 3H). ESIMS m/z 290 $(MH)^+$.

*N-(4-Chlorophenyl)-5-methyl-2-(methyloxy)[1,2,4]triazolo[1,5-a]pyrimidin-7-amine (****67****).* White solid (57% yield). ^{1}H NMR (300 MHz, DMSO-d_6) δ ppm: 10.25–9.96 (br, 1H), 7.55–7.49 (m, 2H), 7.49–7.42 (m, 2H), 6.38 (s, 1H), 4.05 (s, 3H), 2.37 (s, 3H). ESIMS m/z 290 $(MH)^+$.

*N-(3-Chlorophenyl)-2-(ethyloxy)-5-methyl[1,2,4]triazolo[1,5-a]pyrimidin-7-amine (****68****).* White solid (74% yield). ^{1}H NMR (300 MHz, DMSO-d_6) δ ppm: 10.42–9.97 (br, 1H), 7.52–7.40 (m, 3H), 7.37–7.34 (m, 1H), 6.43 (s, 1H), 4.46 (q, J = 7.1 Hz, 2H), 2.39 (s, 3H), 1.39 (t, J = 7.1 Hz, 3H). ESIMS m/z 304 $(MH)^+$.

*N-(4-Chlorophenyl)-2-(ethyloxy)-5-methyl[1,2,4]triazolo[1,5-a]pyrimidin-7-amine (****69****).* White solid (74% yield). ^{1}H NMR (300 MHz, DMSO-d_6) δ ppm: 10.24–9.99 (br, 1H), 7.54–7.52 (m, 2H), 7.47–7.43 (m, 2H), 6.38 (s, 1H), 4.46 (q, J = 7.0 Hz, 2H), 2.37 (s, 3H), 1.39 (t, J = 7.0 Hz, 3H). ESIMS m/z 304 $(MH)^+$.

*2-(Ethyloxy)-5-methyl-N-[4-(trifluoromethyl)phenyl][1,2,4]triazolo-[1,5-a]pyrimidin-7-amine (****70****).*[42] Beige solid (66% yield). ^{1}H NMR (300 MHz, $CDCl_3$) δ ppm: 7.79–7.71 (br, 3H), 7.46 (d, J = 8.3 Hz, 2H), 6.47 (s, 1H), 4.56 (q, J = 7.1 Hz, 2H), 2.55 (s, 3H), 1.49 (t, J = 7.1 Hz, 3H). ESIMS m/z 338 $(MH)^+$.

*2-(Ethyloxy)-5-methyl-N-[4-(pentafluoro-λ^6-sulfanyl)phenyl][1,2,4]triazolo[1,5-a]pyrimidin-7-amine (****71****).*[42] White solid (41% yield). ^{1}H NMR (300 MHz, $CDCl_3$) δ ppm: 7.91–7.85 (m, 2H), 7.82–7.76 (br, 1H), 7.43 (d, J = 8.8 Hz, 2H), 6.51 (s, 1H), 4.56 (q, J = 7.1 Hz, 2H), 2.56 (s, 3H), 1.49 (t, J = 7.1 Hz, 3H). ESIMS m/z 396 $(MH)^+$.

*N-(4-Chlorophenyl)-5-methyl-2-{[2-(methyloxy)ethyl]oxy}[1,2,4]triazolo[1,5-a]pyrimidin-7-amine (****72****).* White solid (46% yield). ^{1}H NMR (300 MHz, $CDCl_3$) δ ppm: 7.51–7.49 (m, 2H), 7.33–7.31 (m, 2H), 6.26 (s, 1H), 4.63 (t, J = 4.6 Hz, 2H), 3.71 (d, J = 84.6 Hz, 2H), 3.45 (s, 3H), 2.5 (s, 3H). ESIMS m/z 334 $(MH)^+$.

*N-(3-Chlorophenyl)-5-methyl-2-{[2-(methyloxy)ethyl]oxy}[1,2,4]triazolo[1,5-a]pyrimidin-7-amine (****73****).* White solid (58% yield). ^{1}H NMR (300 MHz, DMSO-d_6) δ ppm: 10.26–9.98 (br, 1H), 7.51–7.47 (m, 2H), 7.43–7.40 (m, 1H), 7.36–7.33 (m, 1H), 6.43 (s, 1H), 4.53–4.51 (m, 2H), 3.71–3.69 (m, 2H), 3.3 (s, 3H), 2.38 (s, 3H). ESIMS m/z 334 $(MH)^+$.

*N-(4-Chlorophenyl)-5-methyl-2-{[2-(methylamino)ethyl]oxy}-[1,2,4]triazolo[1,5-a]pyrimidin-7-amine (****74****).* White solid (61% yield). ^{1}H NMR (300 MHz, DMSO-d_6) δ ppm: 10.05–9.84 (br, 1H), 8.82–8.59 (br, 1H), 7.57–7.5 (m, 2H), 7.47–7.43 (m, 2H), 6.39 (s, 1H), 4.67–4.63 (m, 2H), 3.49–3.37 (br, 2H), 2.68–2.64 (m, 3H), 2.38 (s, 3H). ESIMS m/z 333 $(MH)^+$.

*N-(3-Chlorophenyl)-5-methyl-2-{[2-(methylamino)ethyl]oxy}-[1,2,4]triazolo[1,5-a]pyrimidin-7-amine (****75****).* White solid (38% yield). ^{1}H NMR (300 MHz, DMSO-d_6) δ ppm: 10.09–9.90 (br, 1H), 8.84–8.6 (br, 1H), 7.53–7.48 (m, 2H), 7.44–7.35 (m, 2H), 6.45 (s, 1H), 4.65 (t, J = 4.8 Hz, 2H), 3.56–3.33 (br, 2H), 2.68–2.64 (m, 3H), 2.40 (s, 3H). ^{1}H NMR (300 MHz, $CDCl_3$) δ ppm: 10.36–9.91 (br, 2H), 7.44–7.27 (m, 4H), 6.18 (s, 1H), 4.99–4.78 (br, 2H), 3.7–3.49 (br, 2H), 2.91 (s, 3H), 2.32 (s, 3H). ESIMS m/z 333 $(MH)^+$.

*5-Methyl-2-{[2-(methylamino)ethyl]oxy}-N-[4-(trifluoromethyl)-phenyl][1,2,4]triazolo[1,5-a]pyrimidin-7-amine (**76**).* White solid (48% yield). ^{1}H NMR (300 MHz, DMSO-d_6) δ ppm: 10.25−10.15 (br, 1H), 8.82−8.6 (br, 1H), 7.84−7.81 (m, 2H), 7.65 (d, J = 8.5 Hz, 2H), 6.64 (s, 1H), 4.68−4.64 (m, 2H), 3.64−3.26 (br, 2H), 2.68−2.64 (m, 3H), 2.42 (s, 3H). ESIMS m/z 367 $(MH)^+$.

*5-Methyl-2-{[2-(methylamino)ethyl]oxy}-N-[4-(pentafluoro-λ^6-sulfanyl)phenyl][1,2,4]triazolo[1,5-a]pyrimidin-7-amine (**77**).* White solid (25% yield). ^{1}H NMR (300 MHz, $CDCl_3$) δ ppm: 9.92−9.67 (br, 2H), 7.88−7.86 (m, 2H), 7.55 (d, J = 8.6 Hz, 2H), 6.34 (s, 1H), 4.93−4.82 (m, 2H), 3.70−3.51 (br, 2H), 2.96−2.84 (br, 3H), 2.43 (s, 3H). ESIMS m/z 425 $(MH)^+$.

*N-(4-Chlorophenyl)-2-{[2-(dimethylamino)ethyl]oxy}-5-methyl-[1,2,4]triazolo[1,5-a]pyrimidin-7-amine (**78**).* White solid (20% yield). ^{1}H NMR (300 MHz, $CDCl_3$) δ ppm: 13.26−11.23 (br, 1H), 7.52−7.46 (m, 2H), 7.36−7.34 (m, 2H), 6.26 (s, 1H), 4.9−4.88 (m, 2H), 3.66−3.64 (m, 2H), 3.00 (s, 6H), 2.51 (s, 3H). ESIMS m/z 347 $(MH)^+$.

*N-(3-Chlorophenyl)-2-{[2-(dimethylamino)ethyl]oxy}-5-methyl-[1,2,4]triazolo[1,5-a]pyrimidin-7-amine (**79**).* White solid (38% yield). ^{1}H NMR (300 MHz, $CDCl_3$) δ ppm: 7.46−7.4 (m, 2H), 7.36−7.27 (m, 2H), 6.34 (s, 1H), 4.9−4.88 (m, 2H), 3.66−3.64 (m, 2H), 2.97 (s, 6H), 2.53 (s, 3H), ESIMS m/z 347 $(MH)^+$.

*2-{[2-(Dimethylamino)ethyl]oxy}-5-methyl-N-[4-(trifluoromethyl)-phenyl][1,2,4]triazolo[1,5-a]pyrimidin-7-amine (**80**).* White solid (7% yield). ^{1}H NMR (300 MHz, $CDCl_3$) δ ppm: 7.76 (d, J = 8.6 Hz, 2H), 7.53 (d, J = 8.6 Hz, 2H), 6.47 (s, 1H), 4.93−4.91 (m, 2H), 3.63 (t, J = 4.9 Hz, 2H), 2.99 (s, 6H), 2.55 (s, 3H). ESIMS m/z 381 $(MH)^+$.

*2-{[2-(Dimethylamino)ethyl]oxy}-5-methyl-N-[4-(pentafluoro-λ^6-sulfanyl)phenyl][1,2,4]triazolo[1,5-a]pyrimidin-7-amine (**81**).* White solid (13% yield). ^{1}H NMR (300 MHz, $CDCl_3$) δ ppm: 7.88 (d, J = 8.8 Hz, 2H), 7.51 (d, J = 8.6 Hz, 2H), 6.51 (s, 1H), 4.92 (t, J = 5.1 Hz, 2H), 3.61 (t, J = 5.1 Hz, 2H), 2.97 (s, 6H), 2.56 (s, 3H). ESIMS m/z 439 $(MH)^+$.

*2-[(2-Aminoethyl)oxy]-N-(3-chlorophenyl)-5-methyl[1,2,4]triazolo-[1,5-a]pyrimidin-7-amine (**82**).* White solid (54% yield). ^{1}H NMR (300 MHz, DMSO-d_6) δ ppm: 10 (s, 1H), 8.05 (br, 2H), 7.53−7.49 (m, 2H), 7.44−7.42 (m, 1H), 7.38−7.36 (m, 1H), 6.44 (s, 1H), 4.59 (t, J = 4.9 Hz, 2H), 3.35−3.31 (m, 2H), 2.39 (s, 3H). ESIMS m/z 319 $(MH)^+$.

*2-[(2-Aminoethyl)oxy]-5-methyl-N-[4-(trifluoromethyl)phenyl]-[1,2,4]triazolo[1,5-a]pyrimidin-7-amine (**83**).* White solid (46% yield). ^{1}H NMR (300 MHz, DMSO-d_6) δ ppm: 10.35−10.08 (br, 1H), 8.06 (br, 2H), 7.83 (d, J = 8.6 Hz, 2H), 7.67−7.65 (m, 2H), 6.63 (s, 1H), 4.61−4.56 (m, 2H), 3.35- 3.31 (m, 2H), 2.41 (s, 3H). ESIMS m/z 353 $(MH)^+$.

*2-[(2-Aminoethyl)oxy]-N-(4-chlorophenyl)-5-methyl[1,2,4]triazolo-[1,5-a]pyrimidin-7-amine (**84**).* White solid (18% yield). ^{1}H NMR (300 MHz, DMSO-d_6) δ ppm: 9.97 (s, 1H), 8.04 (br, 2H), 7.54 (d, J = 8.6 Hz, 2H), 7.45 (d, J = 8.6 Hz, 2H), 6.39 (s, 1H), 4.59 (t, J = 4.9 Hz, 2H), 3.34−3.31 (m, 2H), 2.37 (s, 3H). ESIMS m/z 319 $(MH)^+$.

*General Procedures for the Synthesis of Compounds **85**−**86**.* These compounds were obtained as a byproduct in the reaction yielding **78**−**79**, probably due to the presence of NaOH in the reaction medium.

*7-[(4-Chlorophenyl)amino]-5-methyl[1,2,4]triazolo[1,5-a]pyrimidin-2(1H)-one (**85**).* White solid (21% yield). ^{1}H NMR (300 MHz, DMSO-d_6) δ ppm: 10.09 (br s, 1H), 7.51 (d, J = 8.8 Hz, 2H), 7.42 (d, J = 8.8 Hz, 2H), 6.44 (br s, 1H), 5.75 (s, 1H), 2.32 (s, 3H). ^{1}H NMR (300 MHz, DMSO-d_6 + D_2O) δ ppm: 7.51−7.49 (m, 2H), 7.42 (d, J = 8.8 Hz, 2H), 6.45 (s, 1H), 5.73 (s, 1H), 2.32 (s, 3H). ESIMS m/z 276 $(MH)^+$.

*7-[(3-Chlorophenyl)amino]-5-methyl[1,2,4]triazolo[1,5-a]pyrimidin-2(1H)-one (**86**).* White solid (38% yield). ^{1}H NMR (300 MHz, DMSO-d_6) δ ppm: 10.16 (br s, 1H), 7.50−7.46 (m, 2H), 7.41−7.39 (m, 1H), 7.35−7.33 (m, 1H), 6.49 (s, 1H), 5.76 (s, 1H), 2.34 (s, 3H). ^{1}H NMR (300 MHz, DMSO-d_6 + D_2O) δ ppm: 7.50−7.46 (m, 2H), 7.39−7.33 (m, 2H), 6.48 (s, 1H), 5.69 (s, 1H), 2.33 (s, 3H). ESIMS m/z 276 $(MH)^+$.

*General Procedures for the Synthesis of **89**−**97** (Scheme 3).* The corresponding amine (10 equiv) in MeOH or THF was added to a solution of the corresponding 2-(chloromethyl) triazolopyrimidine derivative (intermediates **45a,b** or **46a,b**) (1 mmol) in tetrahydrofuran (THF) (6 mL). The mixture was heated under microwave irradiation at 120 °C for 30−45 min. Whenever reaction completion had not been reached, more amine in MeOH or THF (10 mmol) was added. The mixture was microwave irradiated at 120 °C until reaction completion had been reached. The mixture was then filtered, and solvent was removed under reduced pressure. The crude mixture was purified by preparative HPLC (SunFire 19 m × 150 mm, H_2O 0.1% TFA−ACN 0.1% TFA gradient from 10 to 100%). Upon freeze-drying of the corresponding fractions, desired product was obtained.

*N-(4-Chlorophenyl)-5-methyl-2-[2-(methylamino)ethyl][1,2,4]-triazolo[1,5-a]pyrimidin-7-amine (**89**).* White solid (68% yield). ^{1}H NMR (400 MHz, DMSO-d_6) δ ppm: 9.57 (br s, 1H), 7.53 (d, J = 7.3 Hz, 2H), 7.47 (d, J = 7.3 Hz, 2H), 6.42 (s, 1H), 3.33 (s, 3H), 3.32−3.27 (m, 2H), 2.61−2.33 (m, 4H). ESIMS m/z 317 $(MH)^+$.

*2-(Aminomethyl)-N-(4-chlorophenyl)-5-methyl-[1,2,4]triazolo-[1,5-a]pyrimidin-7-amine (**90**).* White solid (16% yield). ^{1}H NMR (300 MHz, $CDCl_3$) δ ppm: 9.52−8.38 (br, 2H), 7.35 (d, J = 8.6 Hz, 2H), 7.30−7.27 (m, 2H), 6.20 (s, 1H), 4.53 (br s, 2H), 2.46 (s, 3H). ESIMS m/z 289 $(MH)^+$.

*N-(4-Chlorophenyl)-5-methyl-2-((methylamino)methyl)-[1,2,4]-triazolo[1,5-a]pyrimidin-7-amine (**91**).* White solid (71% yield). ^{1}H NMR (300 MHz, $CDCl_3$) δ ppm: 10.61−9.65 (br, 1H), 7.53−7.44 (m, 4H), 6.24 (s, 1H), 4.40 (s, 2H), 2.97 (s, 3H), 2.49 (s, 3H). ESIMS m/z 303 $(MH)^+$.

*N-(4-Chlorophenyl)-2-((dimethylamino)methyl)-5-methyl-[1,2,4]-triazolo[1,5-a]pyrimidin-7-amine (**92**).* White solid (31% yield). ^{1}H NMR (300 MHz, $CDCl_3$) δ ppm: 7.50−7.47 (m, 2H), 7.41−7.37 (m, 2H), 6.42 (s, 1H), 4.53 (s, 2H), 3.05 (s, 6H), 2.58 (s 3H). ESIMS m/z 317 $(MH)^+$.

*N-(3-Chlorophenyl)-5-methyl-2-[2-(methylamino)ethyl][1,2,4]-triazolo[1,5-a]pyrimidin-7-amine (**93**).* White solid (53% yield). ^{1}H NMR (400 MHz, DMSO-d_6) δ ppm: 9.57 (br s, 1H), 7.53−7.33 (m, 4H), 7.47 (d, J = 7.3 Hz, 2H), 6.48 (s, 1H), 3.33 (s, 3H), 3.23−3.20 (m, 2H), 2.64−2.34 (m, 4H). ESIMS m/z 317 $(MH)^+$.

*N-(3-Chlorophenyl)-2-((dimethylamino)methyl)-5-methyl-[1,2,4]-triazolo[1,5-a]pyrimidin-7-amine (**94**).* Pale-yellow solid (56% yield). ^{1}H NMR (300 MHz, $CDCl_3$) δ ppm: 7.46−7.42 (m, 2H), 7.35−7.32 (m, 2H), 6.48 (s, 1H), 4.49 (s, 2H), 3.03 (s, 6H), 2.59 (s 3H). ESIMS m/z 317 $(MH)^+$.

*2-(Aminomethyl)-N-(3-chlorophenyl)-5-methyl-[1,2,4]triazolo-[1,5-a]pyrimidin-7-amine (**95**).* Pale-yellow solid (11% yield). ^{1}H NMR (300 MHz, MeOH-d_4) δ ppm: 7.53−7.50 (m, 2H), 7.43−7.40 (m, 2H), 6.50 (s, 1H), 4.42 (s, 2H), 2.52 (s, 3H). ESIMS m/z 289 $(MH)^+$.

*N-(3-Chlorophenyl)-5-methyl-2-((methylamino)methyl)-[1,2,4]-triazolo[1,5-a]pyrimidin-7-amine (**96**).* White solid (21% yield). ^{1}H NMR (300 MHz, $CDCl_3$) δ ppm: 10.7−10.08 (br, 1H), 7.39−7.32 (m, 2H), 7.28−7.27 (m, 2H), 6.31 (s, 1H), 4.39 (s, 2H), 2.97 (s, 3H), 2.50 (s, 3H). ESIMS m/z 303 $(MH)^+$.

*2-(2-Aminoethyl)-N-(4-chlorophenyl)-5-methyl[1,2,4]triazolo-[1,5-a]pyrimidin-7-amine (**97**).* White solid (40% yield). ^{1}H NMR (400 MHz, DMSO-d_6) δ ppm: 7.77 (br s, 2H), 7.53 (d, J = 7.3 Hz, 2H), 7.47 (d, J = 7.3 Hz, 2H), 6.42 (s, 1H), 3.27 (m, 2H), 3.25 (m, 2H), 2.40 (s, 3H). ESIMS m/z 303 $(MH)^+$.

*General Procedures for the Synthesis of **98** and **99** (Scheme 4).* Palladium 10% on activated charcoal (330.06 mmol) was placed in a hydrogenation flask under N_2 atmosphere; intermediate **47a** or **47b** (1 mmol) dissolved in acetic acid (10 mL) was added. The reaction mixture was hydrogenated at 35 psi and checked at 16, 30, and 40 h. After this time, LCMS showed a mixture of starting material, dehalogenated

starting material, desired product, and dehalogenated desired product in ratio (35/5/50/10). The reaction mixture was concentrated under vacuum and purified by preparative HPLC (SunFire, H_2O 0.1% TFA−ACN 0.1% TFA gradient from 10 to 100%). After collection of the appropriate fractions, solvent was evaporated under reduced pressure and the product was dried under vacuum in presence of phosphorus pentoxide overnight to give the desired product.

*{7-[(4-Chlorophenyl)amino]-5-methyl[1,2,4]triazolo[1,5-a]pyrimidin-2-yl}methanol (**98**).* White solid (11% yield). ^{1}H NMR (400 MHz, DMSO-d_6) δ ppm: 10.52 (br s, 1H), 7.53 (d, J = 8.3 Hz, 2H), 7.46 (d, J = 8.3 Hz, 2H), 6.45 (s, 1H), 4.66 (s, 2H), 2.42 (s, 3H). ESIMS m/z 290 $(MH)^+$.

*{7-[(3-Chlorophenyl)amino]-5-methyl[1,2,4]triazolo[1,5-a]pyrimidin-2-yl}methanol (**99**).* White solid (12% yield). ^{1}H NMR (400 MHz, DMSO-d_6) δ ppm: 10.36 (br s, 1H), 7.52−7.45 (m, 3H), 7.37−7.34 (m, 1H), 6.50 (s, 1H), 4.66 (s, 2H), 2.42 (s, 3H). ESIMS m/z 290 $(MH)^+$.

*Synthesis of Compound **101** (Scheme 4). 5-Methyl-2-{2-[(phenylmethyl)oxy]ethyl}-N-[4-(trifluoromethyl)phenyl][1,2,4]triazolo[1,5-a]pyrimidin-7-amine (**100**).* A suspension of Intermediate **10p** (0.302 g, 0.997 mmol) and 4-(trifluoromethyl)aniline (0.125 mL, 0.997 mmol) in ethanol (5 mL) was heated at 50 °C for 1 h. The reaction mixture was concentrated under vacuum, taken up with DCM (20 mL), and washed with Na_2CO_3 (2 × 15 mL). The organic layer was dried over anhydrous Na_2SO_4 filtered and concentrated under vacuum to afford a pale-yellow solid (0.407 g, 95% yield). ^{1}H NMR (300 MHz, DMSO-d_6) δ ppm: 10.02 (s, 1H), 7.79 (d, J = 8.6 Hz, 2H), 7.67 (d, J = 8.6 Hz, 2H), 7.32−7.25 (m, 5H), 6.61 (s, 1H), 4.51 (s, 2H), 3.90 (t, J = 6.6 Hz, 2H), 3.10 (t, J = 6.6 Hz, 2H), 2.42 (s, 3H). ESIMS m/z 428 $(MH)^+$.

*2-(5-Methyl-7-{[4-(trifluoromethyl)phenyl]amino}[1,2,4]triazolo-[1,5-a]pyrimidin-2-yl)ethanol (**101**).* A solution of Intermediate **100** (0.25 g, 0.585 mmol) in methanol (3 mL) was hydrogenated using 10% Pd/C as catalyst. The reaction mixture was concentrated, and the residue was purified by flash chromatography (silica gel column, eluting with DCM:MeOH mixtures from 100:0 to 90:10%). Upon collection of the appropriate fractions, the title compound was obtained as a white solid (0.055 g, 30% yield). ^{1}H NMR (400 MHz, DMSO-d_6) δ ppm: 10.40 (s, 1H), 7.80 (d, J = 8.6 Hz, 2H), 7.67 (d, J = 8.6 Hz, 2H), 6.60 (s, 1H), 4.72 (t, J = 5.5 Hz, 1H), 3.85 (q, J = 6.8 Hz, 2H), 2.96 (t, J = 6.8 Hz, 2H), 2.43 (s, 3H), ESIMS m/z 338 $(MH)^+$.

■ ASSOCIATED CONTENT

Ⓢ Supporting Information. Table of synthetic intermediates, table of the crystallographic refinement statistics, and figure of the $F_o - F_c$ difference map. This material is available free of charge via the Internet at http://pubs.acs.org.

Accession Codes

The X-ray structure coordinates for *Pf*DHODH in complex with **37** have been deposited in the Protein Data Bank as PDB ID code 3SFK.

■ AUTHOR INFORMATION

Corresponding Author

*Phone: (214) 645-6164. E-mail: margaret.phillips@UTSouthwestern.edu.

■ ACKNOWLEDGMENT

The team acknowledges Dr. Dennis Kyle for providing the atovaquone resistant lines TM90C2B and TM90C2A, Dr. Akhil Vaidya for providing the D10 cell line harboring yeast DHODH, and Dr. Leonard D. Shultz and The Jackson Laboratory for providing access to NOD-*scid* IL-2Rγ^{null} for the in vivo evaluation of compounds in the *P. falciparum* murine model through collaboration with GlaxoSmithKline. The team also acknowledges Emma Castro and Angel Pajares (Red Cross Blood Bank, Madrid, Spain) for the supply of human erythrocytes to perform the in vivo experiments in the *P. falciparum* murine model. This work was supported by the United States National Institutes of Health grants, U01AI075594 (to M.A.P., P.K.R., S.A.C. and I.B.) and R01AI53680 (to M.A.P. and P.K.R.). M.A.P. acknowledges support of the Welch Foundation (I-1257). and P.K.R. also acknowledges a Grand Challenge Explorations Award from the Bill and Melinda Gates Foundation. M.A.P. holds the Carolyn R. Bacon Professorship in Medical Science and Education.

■ DEDICATION

We would like to dedicate this paper to the memory of our colleague and dear friend Ian Bathurst, whose intelligence, dedication and humor will be greatly missed by all who knew him.

■ ABBREVIATIONS USED

*Pf*DHODH, *P. falciparum* dihydroorotate dehydrogenase; *Pb*DHODH, *P. berghei* DHODH; *Pv*DHODH, *P. vivax* DHODH; *h*DHODH, human DHODH; CoQ, ubiquinone; FMN, flavin mononucleotide; HTS, high throughput screen; ACTs, artemesinin-based combination therapies; ADME, adsorption, distribution, metabolism, excretion; SAR, structure−activity relationships

■ REFERENCES

(1) Meshnick, S. R.; Dobson, M. J. The history of antimalarial drugs. In *Antimalarial Chemotherapy: Mechanisms of Action, Resistance, and New Directions in Drug Discovery*; Rosenthal, P., Ed.; Humana Press Inc: Totowa, NJ, 2001; pp 15−25.

(2) Guerra, C. A.; Gikandi, P. W.; Tatem, A. J.; Noor, A. M.; Smith, D. L.; Hay, S. I.; Snow, R. W. The limits and intensity of *Plasmodium falciparum* transmission: implications for malaria control and elimination worldwide. *PLoS Med.* **2008**, *5*, e38.

(3) Greenwood, B. M.; Fidock, D. A.; Kyle, D. E.; Kappe, S. H.; Alonso, P. L.; Collins, F. H.; Duffy, P. E. Malaria: progress, perils, and prospects for eradication. *J. Clin. Invest.* **2008**, *118*, 1266–1276.

(4) Greenwood, B. M. Control to elimination: implications for malaria research. *Trends Parasitol.* **2008**, *24*, 449–454.

(5) Ballou, W. R. The development of the RTS,S malaria vaccine candidate: challenges and lessons. *Parasite Immunol.* **2009**, *31*, 492–500.

(6) White, N. J. Antimalarial drug resistance. *J. Clin. Invest.* **2004**, *113*, 1084–1092.

(7) Eastman, R. T.; Fidock, D. A. Artemisinin-based combination therapies: a vital tool in efforts to eliminate malaria. *Nature Rev. Microbiol.* **2009**, *7*, 864–874.

(8) Dondorp, A. M.; Yeung, S.; White, L.; Nguon, C.; Day, N. P.; Socheat, D.; von Seidlein, L. Artemisinin resistance: current status and scenarios for containment. *Nature Rev. Microbiol.* **2010**, *8*, 272–280.

(9) Mackinnon, M. J.; Marsh, K. The selection landscape of malaria parasites. *Science* **2010**, *328*, 866–871.

(10) Olliaro, P.; Wells, T. N. The global portfolio of new antimalarial medicines under development. *Clin. Pharmacol. Ther.* **2009**, *85*, 584–595.

(11) Wells, T. N.; Alonso, P. L.; Gutteridge, W. E. New medicines to improve control and contribute to the eradication of malaria. *Nature Rev. Drug Discovery* **2009**, *8*, 879–891.

(12) Craft, J. C. Challenges facing drug development for malaria. *Curr. Opin. Microbiol.* **2008**, *11*, 428–433.

(13) Guiguemde, W. A.; Shelat, A. A.; Bouck, D.; Duffy, S.; Crowther, G. J.; Davis, P. H.; Smithson, D. C.; Connelly, M.; Clark, J.; Zhu, F.; Jimenez-Diaz, M. B.; Martinez, M. S.; Wilson, E. B.; Tripathi, A. K.; Gut, J.; Sharlow, E. R.; Bathurst, I.; El Mazouni, F.; Fowble, J. W.; Forquer, I.; McGinley, P. L.; Castro, S.; Angulo-Barturen, I.; Ferrer, S.; Rosenthal, P. J.; Derisi, J. L.; Sullivan, D. J.; Lazo, J. S.; Roos, D. S.; Riscoe, M. K.; Phillips, M. A.; Rathod, P. K.; Van Voorhis, W. C.; Avery, V. M.; Guy, R. K. Chemical genetics of *Plasmodium falciparum*. *Nature* **2010**, *465*, 311–315.

(14) Gamo, F. J.; Sanz, L. M.; Vidal, J.; de Cozar, C.; Alvarez, E.; Lavandera, J. L.; Vanderwall, D. E.; Green, D. V.; Kumar, V.; Hasan, S.; Brown, J. R.; Peishoff, C. E.; Cardon, L. R.; Garcia-Bustos, J. F. Thousands of chemical starting points for antimalarial lead identification. *Nature* **2010**, *465*, 305–310.

(15) Phillips, M. A.; Rathod, P. K. Plasmodium dihydroorotate dehydrogenase: a promising target for novel anti-malarial chemotherapy. *Infect. Disord. Drug Targets* **2010**, *10*, 226–239.

(16) Gujjar, R.; Marwaha, A.; El Mazouni, F.; White, J.; White, K. L.; Creason, S.; Shackleford, D. M.; Baldwin, J.; Charman, W. N.; Buckner, F. S.; Charman, S.; Rathod, P. K.; Phillips, M. A. Identification of a metabolically stable triazolopyrimidine-based dihydroorotate dehydrogenase inhibitor with antimalarial activity in mice. *J. Med. Chem.* **2009**, *52*, 1864–1872.

(17) Phillips, M. A.; Gujjar, R.; Malmquist, N. A.; White, J.; El Mazouni, F.; Baldwin, J.; Rathod, P. K. Triazolopyrimidine-based dihydroorotate dehydrogenase inhibitors with potent and selective activity against the malaria parasite, *Plasmodium falciparum*. *J. Med. Chem.* **2008**, *51*, 3649–3653.

(18) Baldwin, J.; Michnoff, C. H.; Malmquist, N. A.; White, J.; Roth, M. G.; Rathod, P. K.; Phillips, M. A. High-throughput screening for potent and selective inhibitors of *Plasmodium falciparum* dihydroorotate dehydrogenase. *J. Biol. Chem.* **2005**, *280*, 21847–21853.

(19) Gujjar, R.; El Mazouni, F.; White, K. L.; White, J.; Creason, S.; Shackleford, D. M.; Deng, X.; Charman, W. N.; Bathurst, I.; Burrows, J.; Floyd, D. M.; Matthews, D.; Buckner, F. S.; Charman, S. A.; Phillips, M. A.; Rathod, P. K. Lead-optimization of aryl and aralkyl amine based triazolopyrimidine inhibitors of *Plasmodium falciparum* dihydroorotate dehydrogenase with anti-malarial activity in mice. *J. Med. Chem.* **2011**, *54*, 3935–3949.

(20) Patel, V.; Booker, M.; Kramer, M.; Ross, L.; Celatka, C. A.; Kennedy, L. M.; Dvorin, J. D.; Duraisingh, M. T.; Sliz, P.; Wirth, D. F.; Clardy, J. Identification and characterization of small molecule inhibitors of *Plasmodium falciparum* dihydroorotate dehydrogenase. *J. Biol. Chem.* **2008**, *283*, 35078–35085.

(21) Booker, M. L.; Bastos, C. M.; Kramer, M. L.; Barker, R. H., Jr.; Skerlj, R.; Bir Sidhu, A.; Deng, X.; Celatka, C.; Cortese, J. F.; Guerrero Bravo, J. E.; Krespo Llado, K. N.; Serrano, A. E.; Angulo-Barturen, I.; Jiménez-Díaz, M. B.; Viera, S.; Garuti, H.; Wittlin, S.; Papastogiannidis, P.; Lin, J.; Janse, C. J.; Khan, S. M.; Duraisingh, M.; Coleman, B.; Goldsmith, E. J.; Phillips, M. A.; Munoz, B.; Wirth, D. F.; Klinger, J. D.; Wiegand, R.; Sybertz, E. Novel inhibitors of *Plasmodium falciparum* dihydroorotate dehydrogenase with anti-malarial activity in the mouse model. *J. Biol. Chem.* **2010**, *285*, 33054–33064.

(22) Deng, X.; Gujjar, R.; El Mazouni, F.; Kaminsky, W.; Malmquist, N. A.; Goldsmith, E. J.; Rathod, P. K.; Phillips, M. A. Structural plasticity of malaria dihydroorotate dehydrogenase allows selective binding of diverse chemical scaffolds. *J. Biol. Chem.* **2009**, *284*, 26999–27009.

(23) Erkin, A. V.; Kruitikov, V. I. Formation, structure and heterocyclization of aminoguanidine and ethyl acetoacetate condensation products. *Russ. J. Gral. Chem.* **2009**, *79*, 1204–1209.

(24) Allen, C. F. H.; Beilfuss, H. R.; Burness, D. M.; Reynolds, G. A.; Tinker, J. F.; VanAllan, J. A. *J. Org. Chem.* **1959**, *24*, 787–793.

(25) Yamashkin, S. A.; Kucherenko, N. Y.; Yurovskaya, M. A. *Khim. Geterotsikl. Soedin.* **1997**, 579–597.

(26) Painter, H. J.; Morrisey, J. M.; Mather, M. W.; Vaidya, A. B. Specific role of mitochondrial electron transport in blood-stage *Plasmodium falciparum*. *Nature* **2007**, *446*, 88–91.

(27) Ganesan, S. M.; Morrisey, J. M.; Ke, H.; Painter, H. J.; Laroiya, K.; Phillips, M. A.; Rathod, P. K.; Mather, M. W.; Vaidya, A. B. Yeast dihydroorotate dehydrogenase as a new selectable marker for *Plasmodium falciparum* transfection. *Mol. Biochem. Parasitol.* **2011**, *177*, 29–34.

(28) Jimenez-Diaz, M. B.; Mulet, T.; Viera, S.; Gomez, V.; Garuti, H.; Ibanez, J.; Alvarez-Doval, A.; Shultz, L. D.; Martinez, A.; Gargallo-Viola, D.; Angulo-Barturen, I. Improved murine model of malaria using *Plasmodium falciparum* competent strains and non-myelodepleted NOD-scid IL2Rgammanull mice engrafted with human erythrocytes. *Antimicrob. Agents Chemother.* **2009**, *53*, 4533–4536.

(29) Otwinowski, Z.; Minor, W. Processing of X-ray diffraction data collected in oscillation mode. *Methods Enzymol.* **1997**, *276*, 307–326.

(30) McCoy, A. J. Solving structures of protein complexes by molecular replacement with Phaser. *Acta Crystallogr., Sect. D: Biol. Crystallogr.* **2007**, *63*, 32–41.

(31) Emsley, P.; Cowtan, K. Coot: model-building tools for molecular graphics. *Acta Crystallogr., Sect. D: Biol. Crystallogr.* **2004**, *60*, 2126–2132.

(32) Murshudov, G. N.; Vagin, A. A.; Dodson, E. J. Refinement of macromolecular structures by the maximum-likelihood method. *Acta Crystallogr., Sect. D: Biol. Crystallogr.* **1997**, *53*, 240–255.

(33) Kleywegt, G. J.; Jones, T. A. A super position. *CCP4/ESF-EACBM Newsletter on Protein Crystallography* **1994**, *31*, 9–14.

(34) Holm, L.; Park, J. DaliLite workbench for protein structure comparison. *Bioinformatics* **2000**, *16*, 566–567.

(35) Desjardins, R. E.; Canfield, C. J.; Haynes, J. D.; Chulay, J. D. Quantitative assessment of antimalarial activity in vitro by a semiautomated microdilution technique. *Antimicrob. Agents Chemother.* **1979**, *16*, 710–718.

(36) Jiang, L.; Lee, P.; White, J.; Rathod, P. Potent and selective activity of a combination of thymidine and 1843U89, a folate-based thymidylate synthase inhibitor, against *Plasmodium falciparum*. *Antimicrob. Agents Chemother.* **2000**, *44*, 1047–1050.

(37) Bevan, C. D.; Lloyd, R. S. A high-throughput screening method for the determination of aqueous drug solubility using laser nephelometry in microtiter plates. *Anal. Chem.* **2000**, *72*, 1781–1787.

(38) Valko, K.; Nunhuck, S.; Bevan, C.; Abraham, M. H.; Reynolds, D. P. Fast gradient HPLC method to determine compounds binding to human serum albumin. Relationships with octanol/water and immobilized artificial membrane lipophilicity. *J. Pharm. Sci.* **2003**, *92*, 2236–2248.

(39) Obach, R. S. Prediction of human clearance of twenty-nine drugs from hepatic microsomal intrinsic clearance data: an examination of in vitro half-life approach and nonspecific binding to microsomes. *Drug Metab. Dispos.* **1999**, *27*, 1350–1359.

(40) Davies, B.; Morris, T. Physiological parameters in laboratory animal and humans. *Pharm. Res.* **1993**, *10*, 1093–1095.

(41) Angulo-Barturen, I.; Jimenez-Diaz, M. B.; Mulet, T.; Rullas, J.; Herreros, E.; Ferrer, S.; Jimenez, E.; Mendoza, A.; Regadera, J.; Rosenthal, P. J.; Bathurst, I.; Pompliano, D. L.; Gomez de las Heras, F.; Gargallo-Viola, D. A murine model of falciparum-malaria by in vivo selection of competent strains in nonmyelodepleted mice engrafted with human erythrocytes. *PLoS One* **2008**, *3*, e2252.

(42) Phillips, M. A.; Rathod, P. K.; Charman, S. A.; Floyd, D.; Burrows, J.; Matthews, G.; Marwaha, A.; Gujar, R.; Coteron-Lopez, J. Antimalarial agents that are inhibitors of dihydroorotate dehydrogenase. Patent WO 2011/041304; PCT/US2010/050532, Apr. 7, 2011.